DOE/NE/37967--T7

DE92 004944

DOE/NE Program in Robotics for Advanced Reactors

Contract No. DE-FG02-86NE37967

A Remote Telepresence Robotic System for Inspection and Maintenance of a Nuclear Power Plant

ANNUAL RESEARCH STATUS REPORT UNIVERSITY OF FLORIDA

December 15, 1991

Principal Investigators

Carl D. Crane III
James S. Tulenko

University of Florida
Gainesville, FL 32611

MASTER

DISTRIBUTION OF THIS DOCUMENT IS UNLIMITED

DISCLAIMER

This report was prepared as an account of work sponsored by an agency of the United States Government. Neither the United States Government nor any agency thereof, nor any of their employees, makes any warranty, express or implied, or assumes any legal liability or responsibility for the accuracy, completeness, or usefulness of any information, apparatus, product, or process disclosed, or represents that its use would not infringe privately owned rights. Reference herein to any specific commercial product, process, or service by trade name, trademark, manufacturer, or otherwise does not necessarily constitute or imply its endorsement, recommendation, or favoring by the United States Government or any agency thereof. The views and opinions of authors expressed herein do not necessarily state or reflect those of the United States Government or any agency thereof.

TABLE OF CONTENTS

1991 RESEARCH TEAM MEMBERS

1. PRINCIPALS

Prof. James S. Tulenko
Dr. Carl D. Crane

2. ASSOCIATED FACULTY

Prof. R. Dalton
Dr. J. Duffy

3. PROGRAM SUPPORTED STUDENTS

S.C. Chiang:	Ph.D. student - Autonomous Path Planning for the ATMS
H. Dai:	Ph.D. student - Graphic Software Support; ALMR Modeling Man-machine Interface
D. Roscheleau:	Ph.D. student - Demo Software Support
S. Clifford:	Master's student - 3D Solid Modeling of Argonne West Fuel Processing Facility, using IGRIP
D. Ioannou:	Master's student - Software and Computer Interfaces Between the Sun, Silicon Graphics, and VMX Computers and the Cybermotion Robot
G. Reuter:	Master's student, graduated Summer 1991 - 3-D Sonar Grid; Gyro Based Navigation
T. Heywood:	Master's student, graduated Summer 1991 - Software/Hardware Support
T. McComas:	Master's student, graduated Spring 1991 Radiation Effects; Environmental Hardening
S. Ridgeway:	Master's student - Passive Force Feedback Joystick Controller
R. Jurcyzk:	Master's student - 3-D Visualization
R. Wheeler:	Bachelor's student - Radiation Effects; Environmental Hardening
E. Swilley:	Bachelor's student - Radiation Effects; Environmental Hardening
D. Haddox	Bachelor's student - Argonne Fuel Cycle Facility Modeling, Man-Machine Interface

5. PROGRAM PARTICIPATING STUDENTS

Akram Bou-Ghannam	Ph.D. student, graduated Summer 1991 - A Knowledge-Based Approach to Consistent World Modeling for a Mobile Robot

PRIMARY RESEARCH AREAS

1. ENVIRONMENTAL HARDENING

   - COMPLETE DEVELOPMENT OF ON-LINE MONITORING RADIATION TESTING CHAMBER AND INVESTIGATE METHODS FOR EXTENDING CHIP LIFETIME

2. DATABASE/WORLD MODELING

   - DEVELOPMENT OF 3-D ROBOT KNOWLEDGE/DATABASE (WORLD MODEL) FOR ADVANCED LIQUID METAL REACTOR (ACMP) AND ARGONNE WEST FUEL CYCLE FACILITY

3. MOBILITY/NAVIGATION/MAN-MACHINE INTERFACE

   - DEVELOP INTERFACE FOR CONTROL OF MOBILE SYSTEMS INTEGRATING WORLD MODELING AND SENSED DATA

4. ARTICULATED TRANSPORTER/MANIPULATOR SYSTEM (ATMS) DEVELOPMENT

   - DEVELOP TESTING APPARATUS FOR ATMS

   - REVIEW DESIGN CONCEPTS TO ENSURE BEST DESIGN AS ODETICS SUBCONTRACTOR IS PHASED OUT

1.0 ENVIRONMENTAL HARDENING:

During the reporting period of 1991, the research on environmental hardening of electronic components was concentrated on two subtasks. First, the test facility was to be upgraded to an On-line Testing and Feedback Radiation Facility. Secondly, the chip for computer control of the Cybermotion Robot Sensing System was to be radiation hardened allowing it to survive longer in a radiation field.

1.1 ON-LINE TESTING AND FEEDBACK RADIATION FACILITY:

The tests are carried out in a Cobalt 60 irradiator, shown in Figure 1.1.1, which has a current source strength of 400 curies, a working volume 33.5 cm high x 38.7 cm wide x 44.4 cm deep and a dose rate to our specimens of about 1/2 Krad/min.

The on-line monitoring system has been made operational in the testing facility. The idea behind the on-line system is to operate the MC68008 in a mode that does not execute any code with all address lines floating. The net result is that address line (AO) toggles from a low to high state each time the program counter is incremented by one. Thus a constant frequency square wave is seen at AO. Any deviation above the tolerance limit indicates failure.

Since the irradiation usually extends over long periods of time, it is not possible to manually keep track of frequency changes. A complete on-line monitoring system has thus been developed and makes use of an acquisition card and a personal computer. The acquisition card has been set in the frequency measuring mode and the computer's software detects any deviations in the frequency above the predetermined limits.

The first part of the experiment involves the calibration of the chip when a statistical file is generated regarding the particular chip. The procedure takes around 45 minutes and can be done any time before the irradiation experiment. When the experiment begins, the software reads

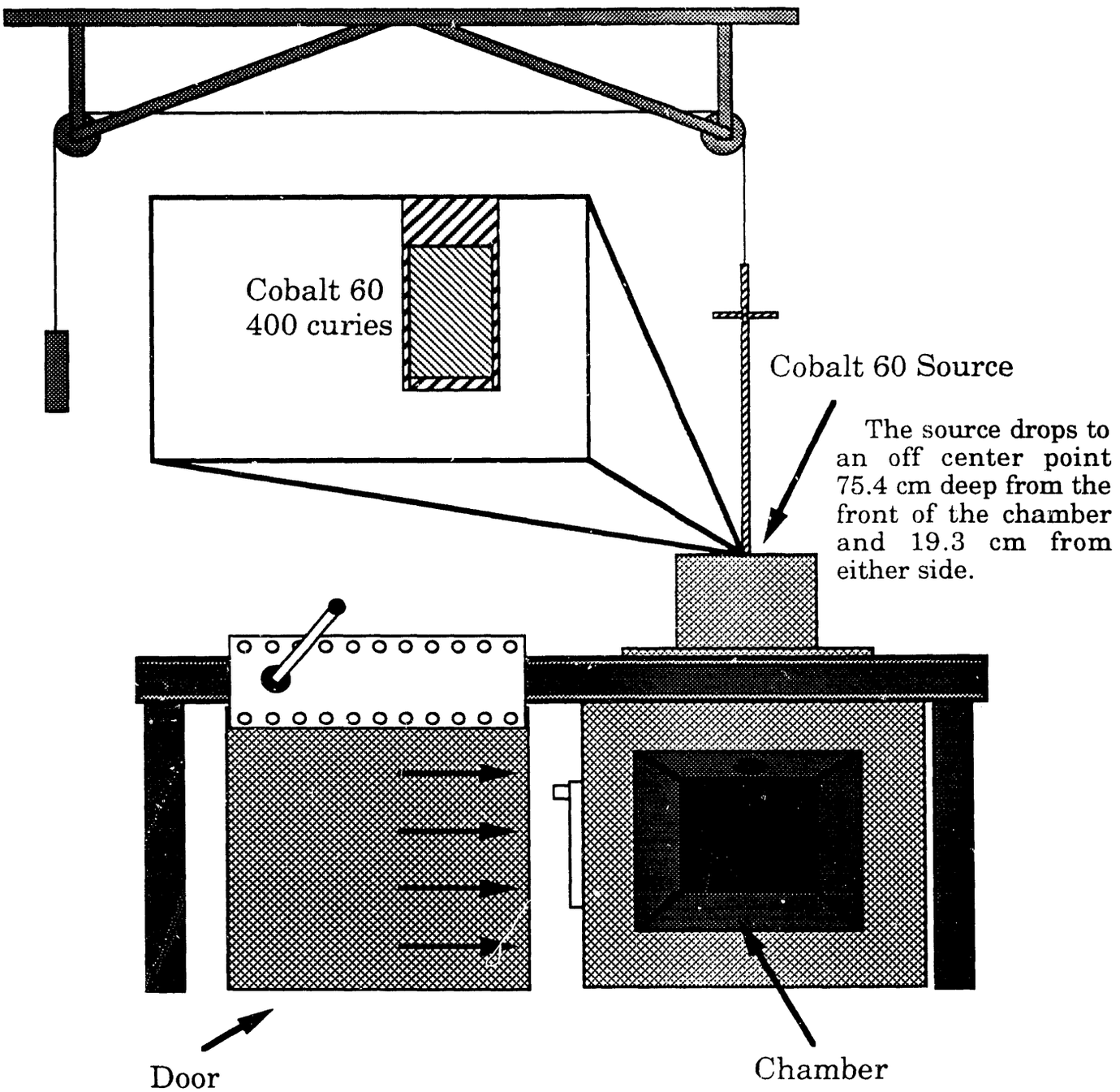

Figure 1.1.1

The Cobalt 60 Irradiator

the value of the incoming frequency and checks with the statistical file for any major deviations. Failure due to radiation damage beyond a certain point will change the output frequency and thus the computer will record the time of failure.

At the end of the experiment information is produced giving the time of failure. The experimental procedure is completely automated other than a flip of a switch which has to be done manually to reset (restart) the microprocessor.

The operating instructions are as follows:

1. Switch on the CRO (scope).
2. Take a probe and connect the CRO to pin No. 46 of the MC68008.
3. Switch on the computer.
4. AT the appearance of the "OK" symbol, press F3. The screen should now show

   "LOAD"

5. Type out the following and press return

   c:\RADHARD\RADHDV10.BAS"

6. Press F2. The screen will ask you now to enter

   (a) Chip type: (you can enter MC68008 for e.g.)

   (b) Chip ID No: (you can enter any alphanumeric name but it should begin with a alphabet. Use this filename to access the output data later)

   (c) Pin No: Enter 46 if monitoring AO)

   (d) No. of update intervals: (you can enter 7 for e.g.,)

   The screen will not give you several menu options.

7. Switch on the power supply and reset the system. A square wave should now be seen on the scope. Choose menu option 3 to calibrate the chip. This will take around 45 minutes.

8. Repeat steps 1 to 6 when you want to begin the experiment. Now select menu option 4 to load the spec file and then press enter to begin the experiment.

9. The output data will be stored in the subdirectory FILES of the directory RADHARD as Chip ID No. dat.

1.2 RADIATION HARDENING OF CYBERMOTION COMPONENTS:

During the course of our environmental research it was noted that when tests were run at the temperatures (260°F) expected to be encountered in reactor containment during a loss-of-coolant accident that electronic components operated twice as long, being able to absorb a factor of over two (twice as much) radiation before failure (Figure 1.2.1) as compared to room temperature electron component radiation failure limit.

The process of annealing (healing) out defects in radiation induced failure by temperature has been well researched. Going back to elementary principles, ionizing radiation effects semiconductor performance by generating electrons (negative charges) and holes (positive charges) in the silicon dioxide of the semi-conductor. The effect of these generated charges as they migrate through the semi-conductor device is to eventually set up a countervailing voltage which negates the operating voltage of the semi-conductor and renders the semi-conductor inoperable. Under a loaded (bias) condition, the electrons that do not quickly recombine with the holes are swept by the voltage through the silica into the material interfaces, leaving the holes behind. This separation leads to eventual semi-conductor failure. Representative values for mobility at room temperature in SiO_2 of the electrons and holes is 20 cm^2/Vs for electrons and $2 \times 10^{-5} cm^2/Vs$ for holes. When

Figure 1.2.1 **MC 68008 Initial Test Results**

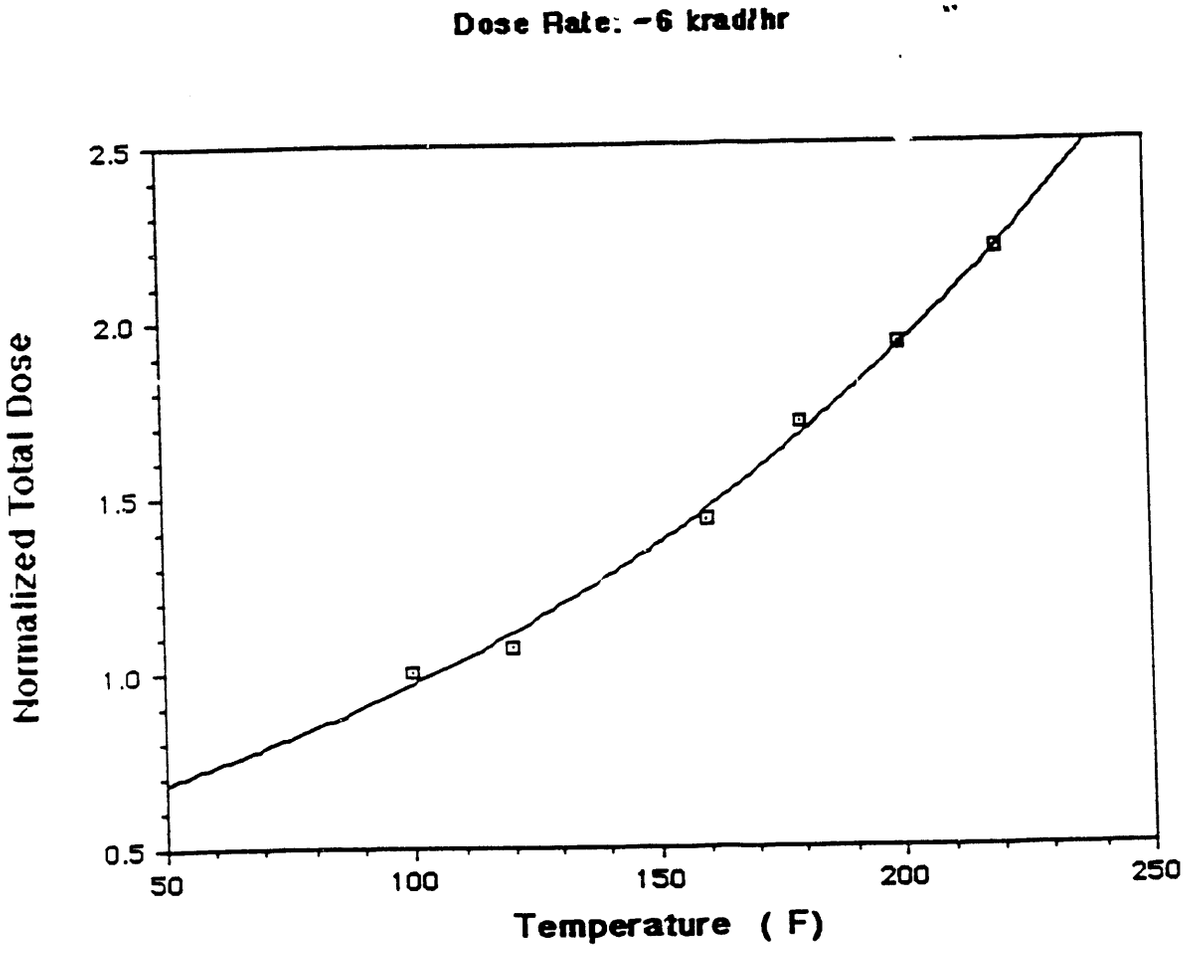

a voltage is applied, the electrons are quickly swept away from the holes preventing the annealing of the defects by the free electrons. Applied thermal heat creates electron motion. Our temperature test results (Figure 1.2.1) showed that the radiation defects are removed, most probably, by the filling in of the positive holes. The radiation damage testing facility developed by the University of Florida allows us to monitor electronic component performance under irradiation while subjecting the chip to varying environmental changes. These temperature annealing results were reported by the Florida Team at the Fourth Topical Meeting on Robotics and Remote Systems during 1991.

We further investigated the use of a high frequency alternating current as an alternate annealing technique to temperature anneal which we feel can be more easily utilized on board a mobile robot. In a manner similar to thermal annealing, we want to investigate the possibility that a high frequency A.C. current makes electrons available to anneal (fill in) the electronic holes. We have run preliminary experiments shown in Figure 1.2.2 with a medium frequency (~ 40 megahertz) alternating current generator upon the same type of chip whose life was extended by the thermal annealing process. One half normal lifetime operation in a radiation field (~nine (9) minutes), followed by annealing for an hour with an ~40 megahertz - A.C. current, increased the radiation failure threshold level by 50%, from 10,000 rads to 15,000 rads. We felt that these results show that our concept had promise. We monitored the temperature used in the circuit resulting from the A.C. 40 megahertz anneal and repeated the experiments using a thermally anneal to the same temperature ~120°F and found the same annealing effect. Our group concludes that the 40 megahertz effect we are using is a temperature annealing effect. Additionally, when we ran the 40 megahertz A.C. anneal inside of our radiation chamber, we shortened the lifetime of the chip indicating that the A.C. anneal process accelerates the separation of electrons and holes.

Figure 1.2.2 One Hour A.C. Anneal Results

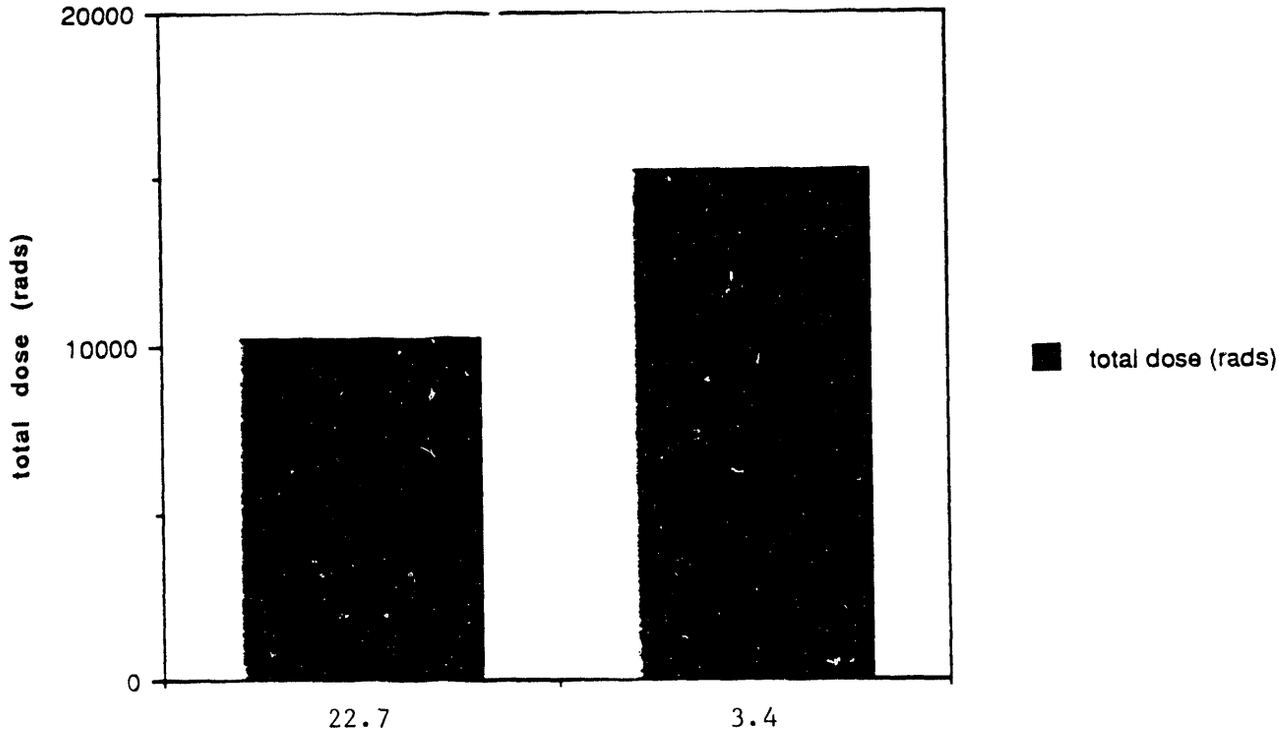

Time till Failure. non-anneal vs. a.c. anneal. Test: 9 min radiation interposed with 1 hrs. control/anneal-repeated until failure

Initially, the 200 megahertz A.C. anneal process was tested on already failed chips. The 200 megahertz annealing technique recovered the chips in one third of the time required by the 40 megahertz anneal process while at the same time causing a much lower temperature in the chip. However, under irradiation the chip recovered by the 200 megahertz anneal failed much faster than the chip recovered by the 40 megahertz anneal. Whereas the 40 megahertz anneal gave consistent results for all four chips run, the 200 megahertz anneal performance ranged from a radiation dose equal to the unannealed control to slightly better than the 40 megahertz, sixty percent improvement. Thus, we currently have received inconsistent results for the 200 megahertz anneal process. At this point we are now intensifying our investigation of the basic radiation damage mechanism occurring in our chips and are also refurbishing our annealing delivery system to ensure we are getting the annealing current to the defected area.

As part of our broad investigation of ways to anneal out radiation defects, we will be investigating, as a minimum, the following mechanisms, in addition to direct heat and to high frequency alternating currents: (1) Hydrogen Gas Diffusion, (2) Radiofrequency (RF) radiation, and (3) Ultra Violet (UV) radiation. Additionally, we will be examining our failed electron components on a microscopic basis to determine the failure mechanisms and will attempt to define additional anneal methods for the particular defect mechanism noted.

2.0 DATABASE/WORLD MODELING

2.1 THE GENERAL ELECTRIC PLANT

During the year 1991 the work on the General Electric Advanced Liquid Metal reactor modeling continued. Florida has been able to import magnetic data files from the 2D AutoCad system used by the architect engineer via the IGSE format from a PC over the network into the IGRIP robotics modeling system on the Silicon Graphics computer. A report has been issued in the form of a technical presentation at the November 1991 American Nuclear Society Meeting. A full technical report including a video tape of the IGRIP model plus a Silicon Graphics tape of all of the pertinent files and an expanded will be shipped to the Oak Ridge Project Office before the end of the year. Figures 2.1.1-2.1.9, on the following pages show views of this work, starting with the Cybermotion robot, importation of AutoCad drawings, construction and deployment of the seismic isolators and construction of an overall view of the reactor, heat exchangers and reactor support building

Using the data supplied at the GE ALMR meeting in San Jose in November 1991 the representation of the reactor support building, with seismic isolators, removal, inspection and replacement will be continued using the IGRIP modeling system. In addition work will be completed on the center of gravity determination for the ALMR in-core sodium heat exchanger. Using the new more detailed data about the reactor container head closure, an animated display of the removal of the heat exchanger through the head will be completed. The first draft is due January 1992 with a final report due July 1992.

2.2 ARGONNE WEST FUEL CYCLE FACILITY

In August of 1991 a visit to the Argonne West Fuel Cycle Division produced information of various parts of the processing facilities in the form of drawings and magnetic copies of the AutoCad versions of these drawings, plus the new furnace being installed in the argon hot cell.

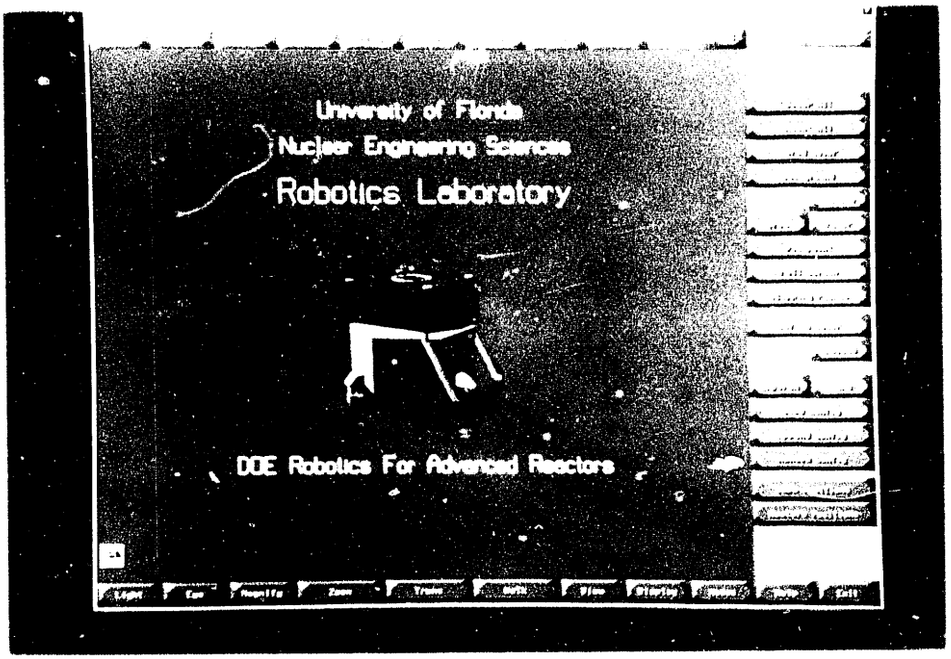
University of Florida
Nuclear Engineering Sciences
Robotics Laboratory
DOE Robotics For Advanced Reactors

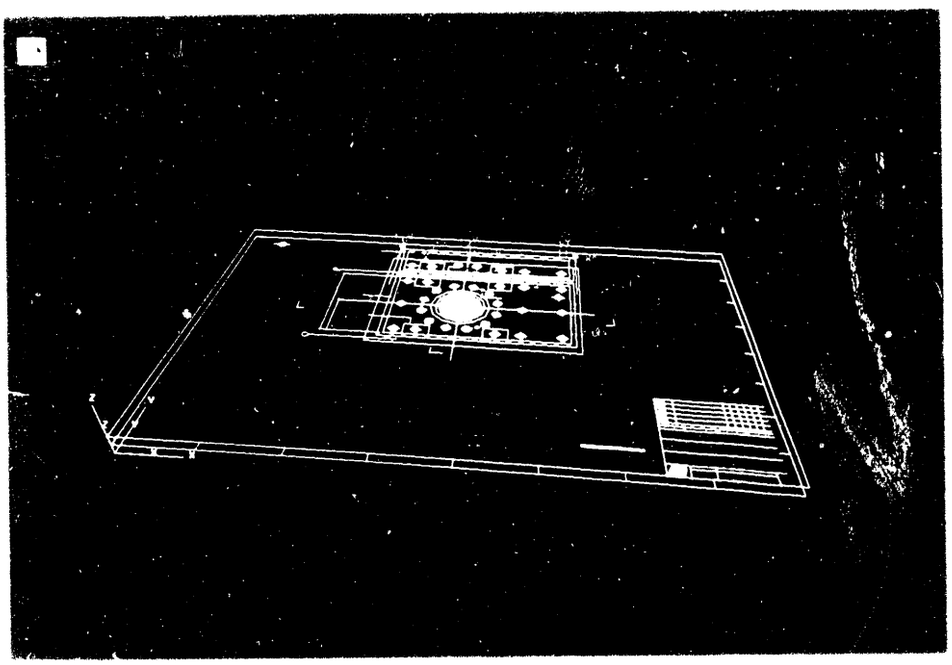

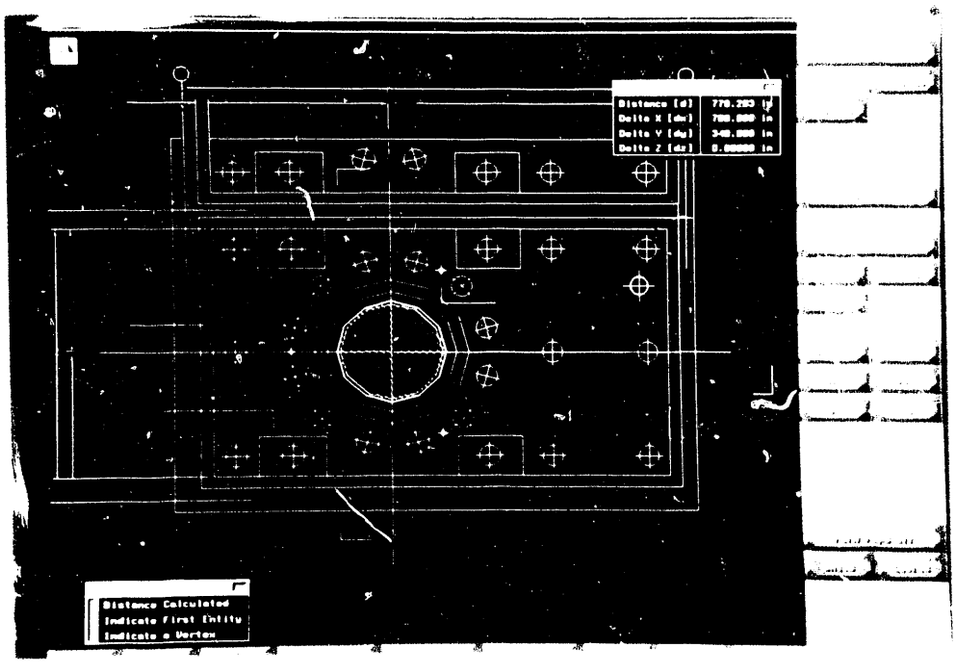
Distance [d]
Delta X [dx]
Delta Y [dy]
Delta Z [dz]
Distance Calculated
Indicate First Entity
Indicate a Vertex

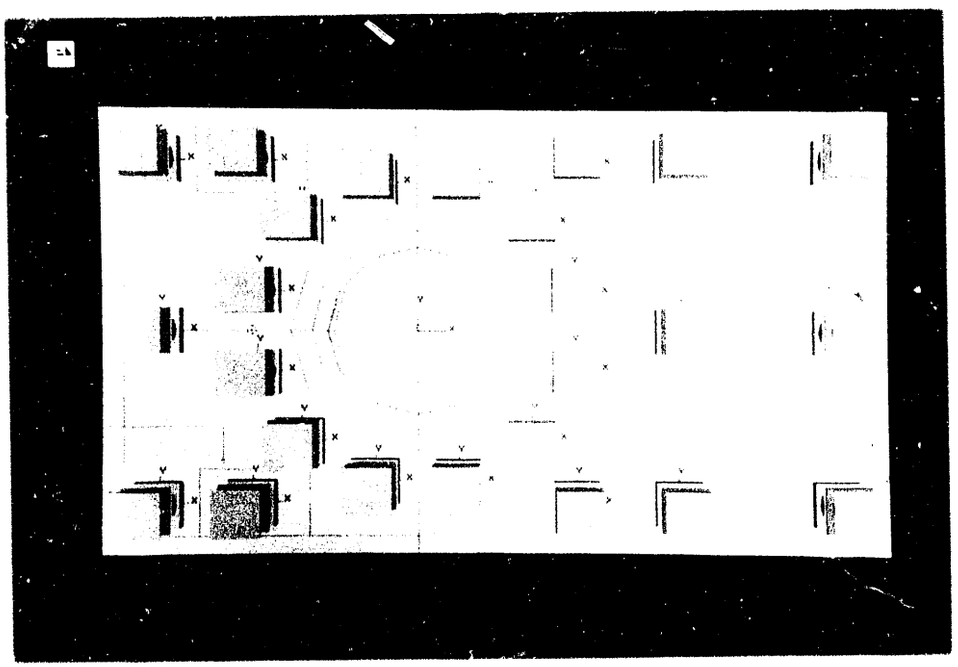

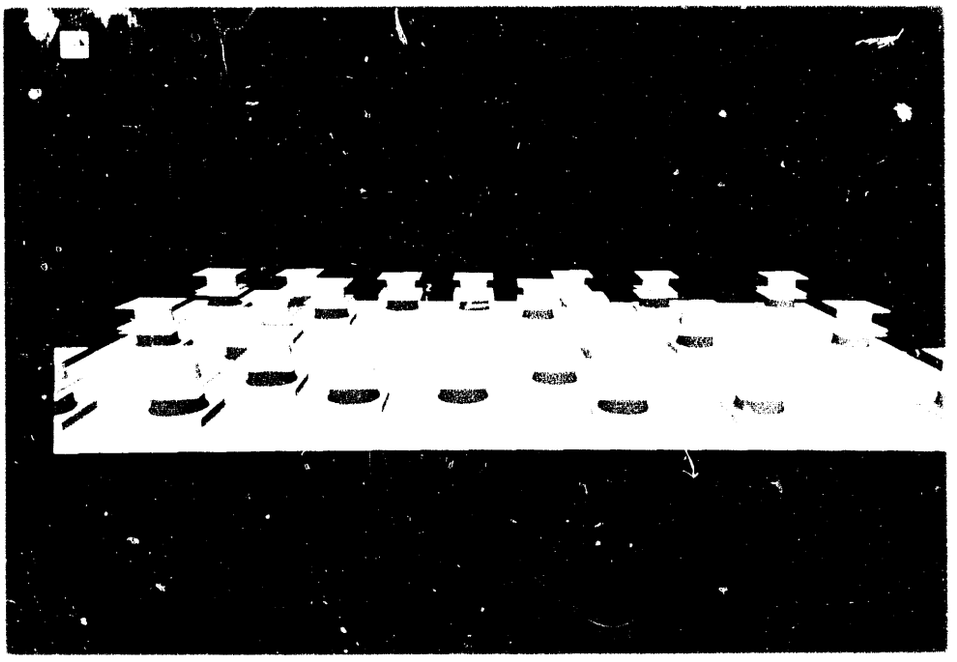

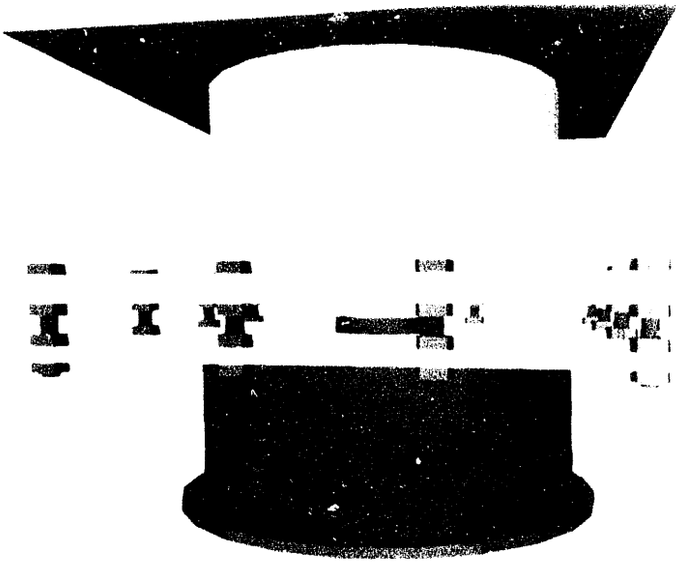

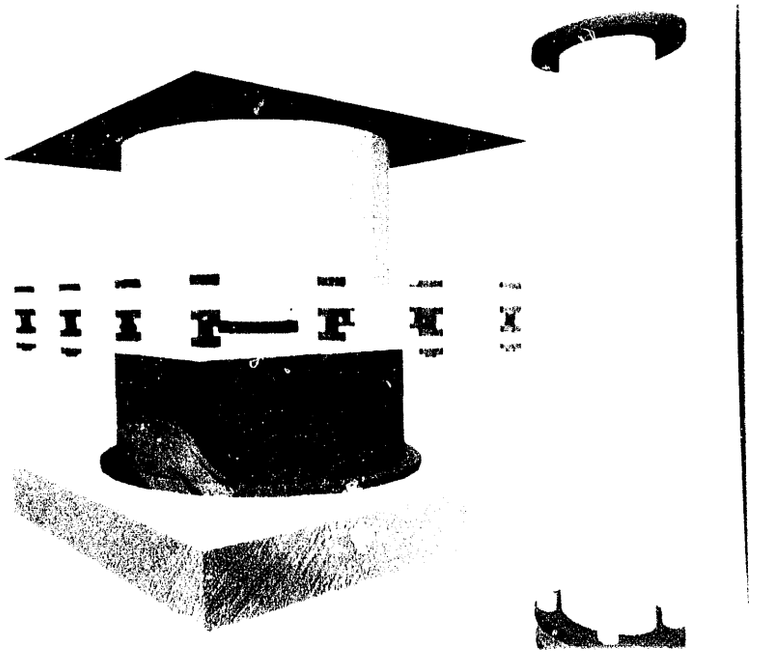

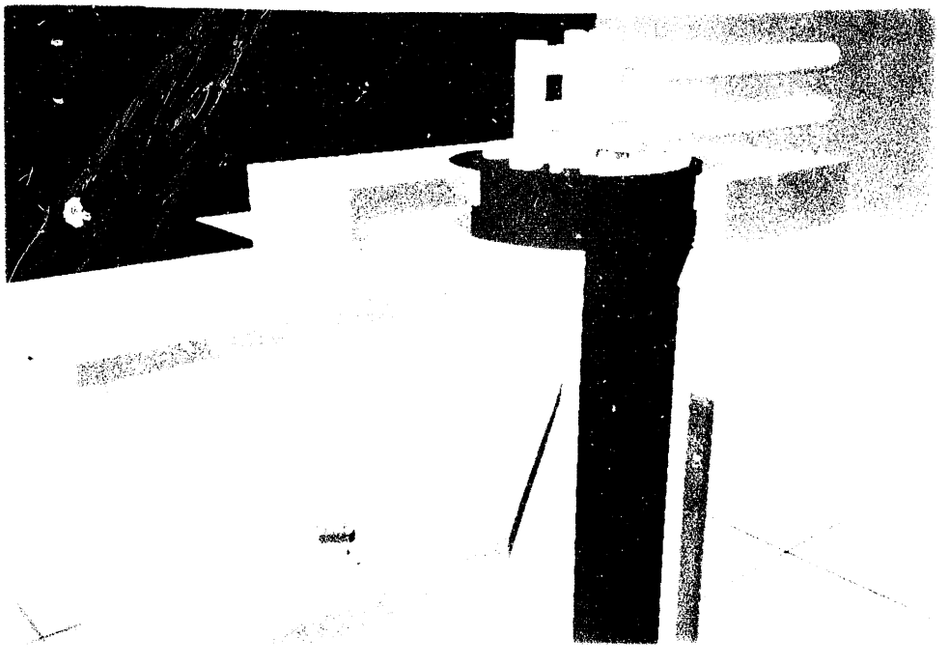

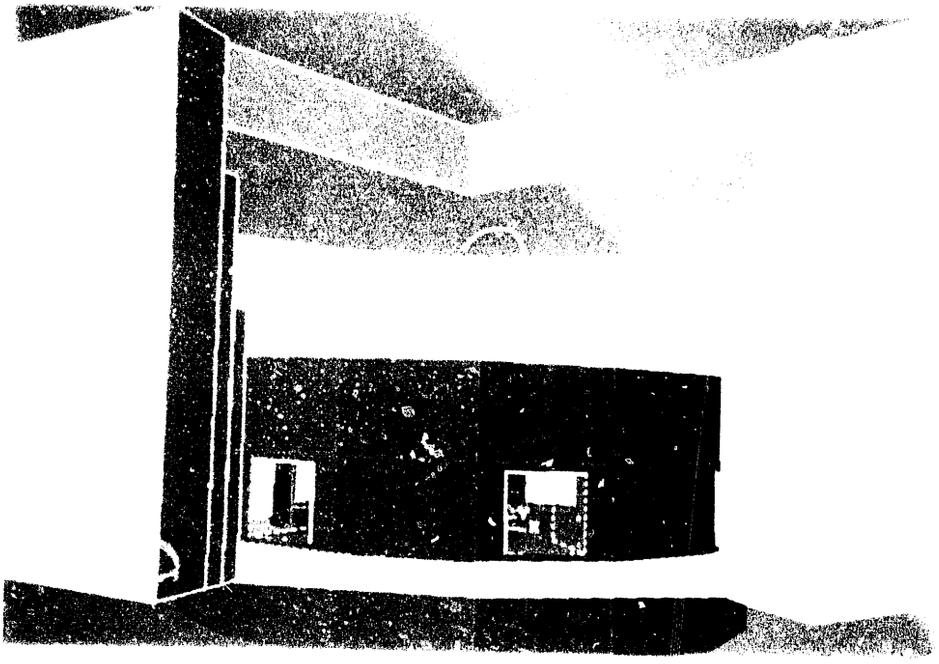

3.1 AUTONOMOUS OPERATION UTILIZING SENSED DATA:

The goal of this task is to enable autonomous operation in a dynamic, unknown, and unstructured indoor environment. The robot has considerable general information about the structure of the environment, but cannot assume that such information is complete. During the year, work was completed in the area of sonar based mapping of an unknown environment. The objective was to determine the coordinates of walls in the mobile robots environment. Also, an objective was to locate doors or gaps in the wall that the mobile robot could investigate further.

The robot system was set up in the indoor lab environment (the Nuclear Engineering Robot Lab) consisting of open space with irregularly shaped boundaries consisting of walls, cabinets, and computer stations. The dimensions of the lab were approximately 8 meters by 5 meters. The floor consisted of smooth tiles necessary for the operation of the wheeled Cybermotion K2A robot. The computational load was distributed over three Silicon Graphics work stations, a personal computer dedicated to the control of the mobile robot, and a sonar sensor system with seven sonar sensors arranged in a semi-circle on top of the mobile robot. The middle sonar sensor points in the forward direction for the robot while the other six sensors are positioned at 30 degree intervals to the right and left of the middle sensor.

The results of our research showed that the system could determine wall locations with accuracy and allow the data to be fed into the knowledge based navigation scheme. Detailed reports are contained in the Doctoral thesis of Dr. Akram Bou-Ghannam and the Masters thesis of Guido Reuter.

4.0 ATMS DEVELOPMENT:

A group was formed at the beginning of 1991 to develop a working version of an ATMS (Articulated Transport Manipulator System). In this year, we have evaluated several ATMS concepts.

4.1 CONCEPTUALIZATIONS AND EVALUATIONS:

Specifications were developed that are believed to meet the requirements of an ATMS in a nuclear reactor type environment.

There are two modes of navigation investigated for the ATMS. The first is horizontal navigation. The second is vertical and bridge navigation. These navigational modes impose the following limits and requirements on the ATMS.

Minimum radius of turn: 610mm (horizontal nav.)

Ascend/descend 40 degrees incline stairs (either or both)

Jump obstacles up to 1m (vertical nav.)

Change elevation: 3m (vertical nav.)

Bridge gaps: 3.6m (bridge nav.)

Navigate speed: 20m/min (horizontal nav.)

Inspection/Manipulation requirements as anticipated as a minimum to be:

Sonar/IR range-proximity sensors

Video

Slave manipulators, either intrinsic or carried along

The navigational requirements were of importance in the design of the ATMS. They limit size and, along with size, set driving force/torque requirements.

Speed requirements set final ratios on wheels, tracks, or other locomotive devices.

Vehicle weight and expected inclines set final driving torque.

Work is ongoing in the further refinement of the present design with emphasis on design objectives.

Elevation change, gaps jumped, obstacles jumped, and vehicle weight set joint torques. For an order of magnitude estimation of joint torques required, simple static modeling of a structure with distributed weight was performed (Figure 4.1.1) for a cantilevered length $\left(M = \frac{w}{2}(\ell - x)^2\right)$ and a suspended length $\left(M = \frac{w}{2}(\ell x - x^2)\right)$

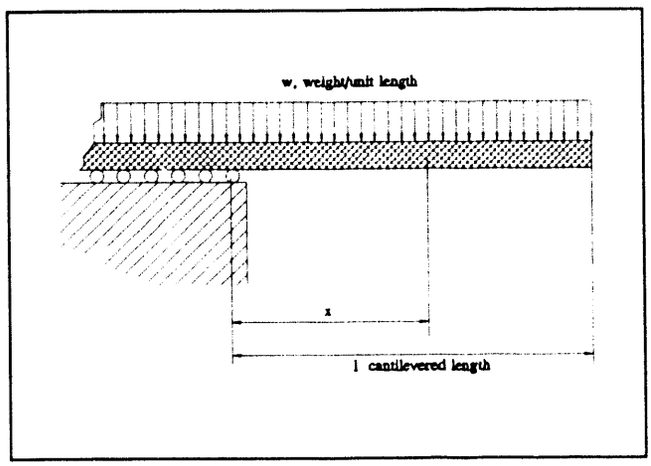

$$M = \frac{w}{2}(l - x)^2$$

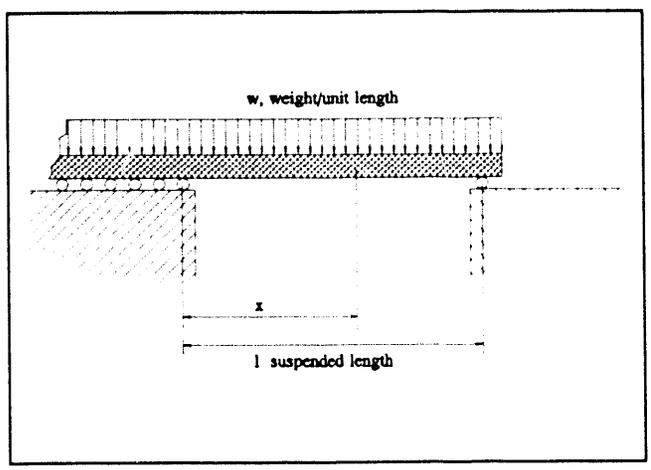

$$M = \frac{w}{2}(lx - x^2)$$

Figure 4.1.1. Joint torque estimation.

Using these rough models and Odetics Inc.'s estimate of a segment's weight of 44.5kg and length of .610 m, order of magnitude was established for joint torque. Length was taken as 3.6 m and w, weight per unit length, was taken as 70 N/m.

Maximum joint torque (quasi static)

cantilever mode	473.6 N-m (40,000 in-lbs)
landed mode	118.4 N-m (10,000 in-lbs)

Note the landed case joint torque is 25% of the cantilevered case. The magnitude of these torques is relatively large. Concepts of joint actuation were considered in light of this requirement.

Radius of turn (for axial center line of ATMS) can be used to set segment length and joint range for the ATMS. A segment with a length of .610 m would require a joint range of $\pm$60 degrees. Some concepts had considerably shorter segment lengths, with corresponding smaller joint range requirements.

4.2 CONCEPTS FOR JOINT ACTUATION CONSIDERED:

1. Serially connected serially actuated segments
2. Pull cable driven
3. Serially connected parallel actuated segments.

A brief description of concepts discussed follows. Power sources vary from hydraulic to electric. Some of the concepts attempt to overcome the joint torque requirements by reducing overall weight. Others allowed for redistribution of weight while undergoing vertical or bridge navigation.

Serially connected serially actuated segments similar to the Odetics Inc. design were examined. Each degree of freedom of this type of joint is actuated by a single prime mover. Estimates of segment weight based on available technology indicated that this concept would be very heavy, if feasible at all. Kinematically, this joint configuration can be modeled with revolutes, either intersecting or non intersecting. Figure 4.2.1 illustrates a chain based on the Hooke joint.

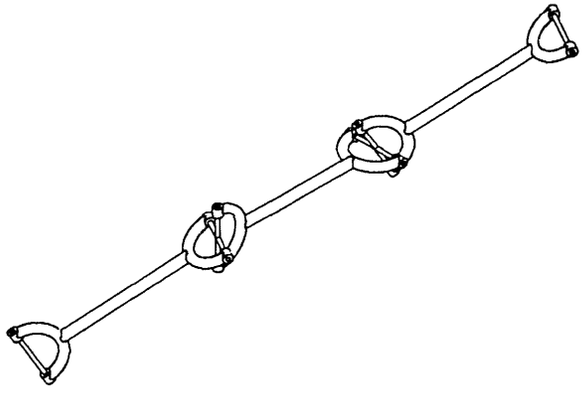

Figure 4.2.1 Serially connected serially actuated joint configuration.

Pull cable driven segments in which a joint is actuated by tensile forces in pull cables located around the joint were examined. The joint could be something as simple as two convex bodies in contact with each other. The concept offers light weight in the segment and joint, but complex and heavy cable drive mechanisms that must also be transported. Sensing of ATMS configuration would be hampered by sliding between convex bodies and cable stretch. Load support of a structure held rigid by tensile and friction forces would be low. Figure 4.2.2 shows a schematic of this type of joint configuration.

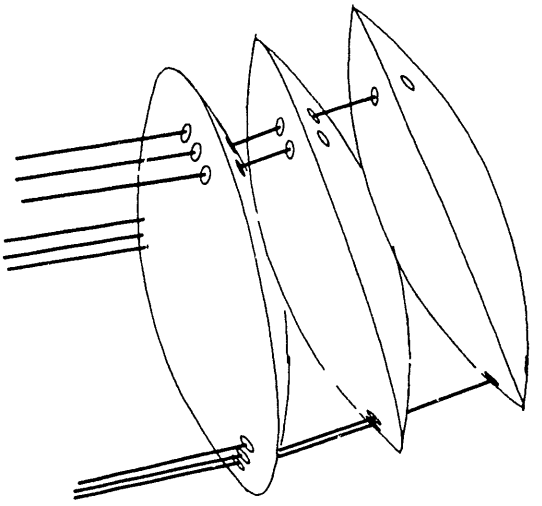

Figure 4.2.2 Pull cable actuated rolling element joint configuration

Serially connected parallel actuated joints were examined. Several types were considered in evolutionary fashion. The first consisted of two joints connected by three

linear actuators and one prismatic joint. Figure 4.2.3 schematically illustrates this joint configuration. There are three degrees of freedom between the two joints. The linear actuators are attached to the joint by Hooke joints. These joints prove difficult to design in compact lightweight versions capable of sustaining expected loads. The linear actuator can be modeled as a cylindrical joint, with the prismatic freedom driven and the rotational freedom free. One feature considered beneficial is the mechanism's ability to stretch.

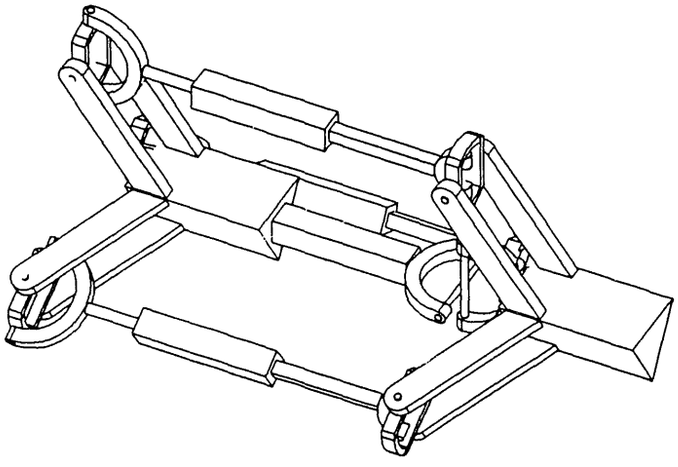

Figure 4.2.3 Parallel actuated joint configuration.

The necessary minimum radius of curvature of the ATMS during horizontal navigation limits the segment length. The vertical and bridge navigational requirements limit weight per length. The ability to stretch or lengthen the distance between joints (reduces weight per length) for vertical navigation and to maintain the minimum length

between joints for horizontal navigation inspired further development of this class of mechanisms.

Axial symmetry was considered. If the ATMS were to fall or become turned over, the ability of the mechanism to right itself is considered important. By removing axial symmetry, mechanism weight could be reduced because horizontal navigation requires less driving torque than horizontal and bridge navigation. It is felt that by removing this symmetry, the ATMS's ability to recover after an upsetting event will be impaired.

A hybrid of the parallel and serial connections was examined in which one rotational degree of freedom was derived from a planar parallel actuation. The planar nature of the parallel actuation allows the linear actuators to be connected by revolute joints. Figure 4.2.4 illustrates this joint configuration. The revolute joint is much simpler to design than a Hooke joint. The serially activated revolute was determined to be a weakness because it would need to carry the moment load.

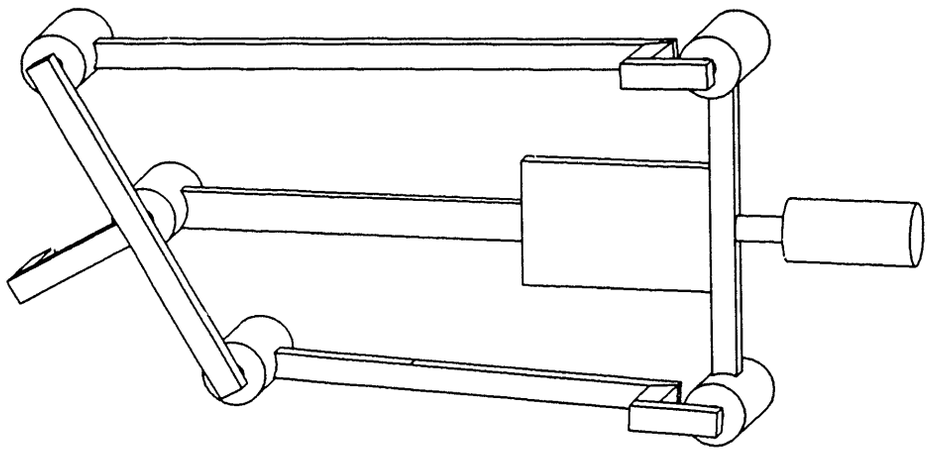

Figure 4.2.4 Parallel planar actuation serial actuation hybrid

The last significant mechanism of this type is one with two degree of freedom parallel planar actuators between joints. The planar actuators are oriented at 90 degrees to each other and are actuating on different joints. This configuration gives each segment four degrees of freedom. Two are collinear sliders and two are orthogonal rotations. The two sliding degrees of freedom allow for large changes in segment length. The planar nature of the actuator leads to revolute connections. A joint has two orthogonal revolutes that can intersect (Hooke joint) or have an offset. Joints are connected to each other by two collinear sliders. Figure 4.2.5 illustrates this joint configuration.

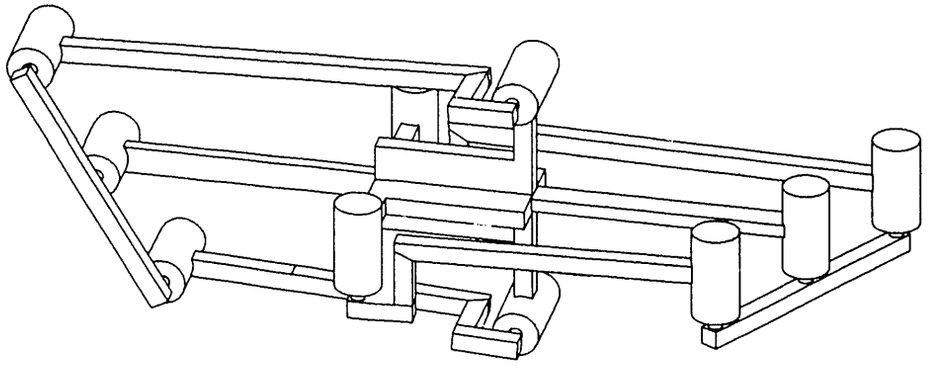

Figure 4.2.5 Orthogonal Parallel planar joint actuation.

Parallel actuation gives rise to a distributed mechanism that can be both light weight and rigid. This type of actuation introduces a sliding degree of freedom that improves

performance in vertical and bridge navigation. These factors lead us to select the final mechanism described for further development and application in ATMS joint actuation.

4.3 HORIZONTAL NAVIGATION:

Methods of locomotion in the horizontal plane were considered as they applied to each joint actuation scheme. Conventional modes are wheels and tracks. These modes could be applied to any of the joint actuation schemes evaluated. The joint actuation schemes with a sliding degree of freedom possess a non-conventional mode of locomotion. This sliding degree of freedom could be utilized in an inchworm-type fashion. But this mode would be difficult to apply in cases of vertical or bridge navigation. Of these modes, wheels, driven and passive, are considered the best for the ATMS. Tracks are more terrain adaptable, but weigh more and add more complexity. The ATMS's terrain is expected to be uniform enough to allow use of wheels. Whether a wheel is driven or not and how and where it is mounted is determined by horizontal navigation requirements and mobility between segments. These issues will be resolved as the mechanical design of the segment joint develops and as horizontal navigation algorithms are developed.

4.4 PHYSICAL REALIZATION OF A PARALLEL ACTUATED ATMS SEGMENT:

Many areas were considered in developing a mechanism that possesses the kinematics previously discussed. Mechanical advantage of the mechanism was examined to size the linear actuators. Weight estimates for the mechanism were made in order to evaluate expected loads. These loads were in turn utilized in component design.

The planar parallel actuator can generate an axial force and a driving torque. The axial force varies with angle and is coupled to slide length through angle. The driving torque varies with angle. This is important because the primary drive required from the parallel actuator is joint torque (Figure 4.4.1).

Given the following notation for the parallel planar actuator:

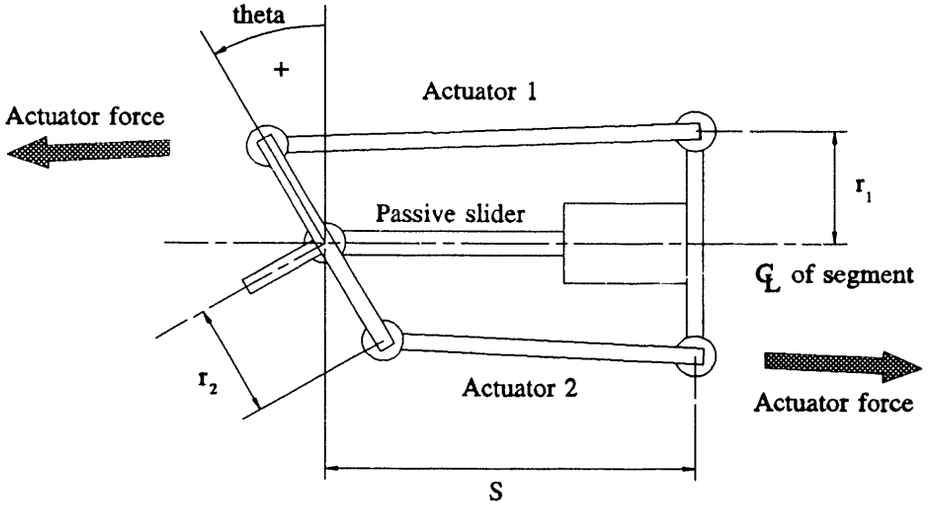

Figure 4.4.1 Parallel planar actuator notation.

equations for the moment generating capacity of the mechanism can be derived. Each actuator contributes to the joint torque. For this discussion, the actuator forces are taken as positive if they generate a right-handed positive joint torque. The equations representing the mechanical advantage of the parallel planar actuator with respect to its moment generating capacity follow.

$$M_a = M_{act1} + M_{act2} \qquad where$$

$$M_{act1} = \frac{r_2}{L_{act1}}(S\cos\theta + r_1\sin\theta) \qquad with$$

$$L_{act1} = ((-r_2\sin\theta - S)^2 + (r_2\cos\theta - r_1)^2)^{\frac{1}{2}}$$

$$M_{act2} = \frac{R_2}{L_{act2}}(S\cos\theta - r_1\sin\theta) \qquad with$$

$$L_{act2} = ((S - r_2\sin\theta)^2 + (-r_1 + r_2\cos\theta)^2)^{\frac{1}{2}}$$

Joint torque as a function of theta has been plotted assuming the actuators can generate a unit force and using geometry that meets ATMS requirements. Figure 8 shows this relationship. For this plot, $r_1 = r_2 = 6.25$ and the slide length S is taken to be 22 in consistent units. A unit force is used to evaluate mechanical advantage.

For the static case, in the vertical plane, the torque necessary to hold a rotating mass at an angular position is a function of the mass's angular displacement from the horizon. This is shown by the curve M_r in figure 4.4.2. In the quasistatic case, vertical navigation of the ATMS will require torques that vary with angle of displacement from the horizon.

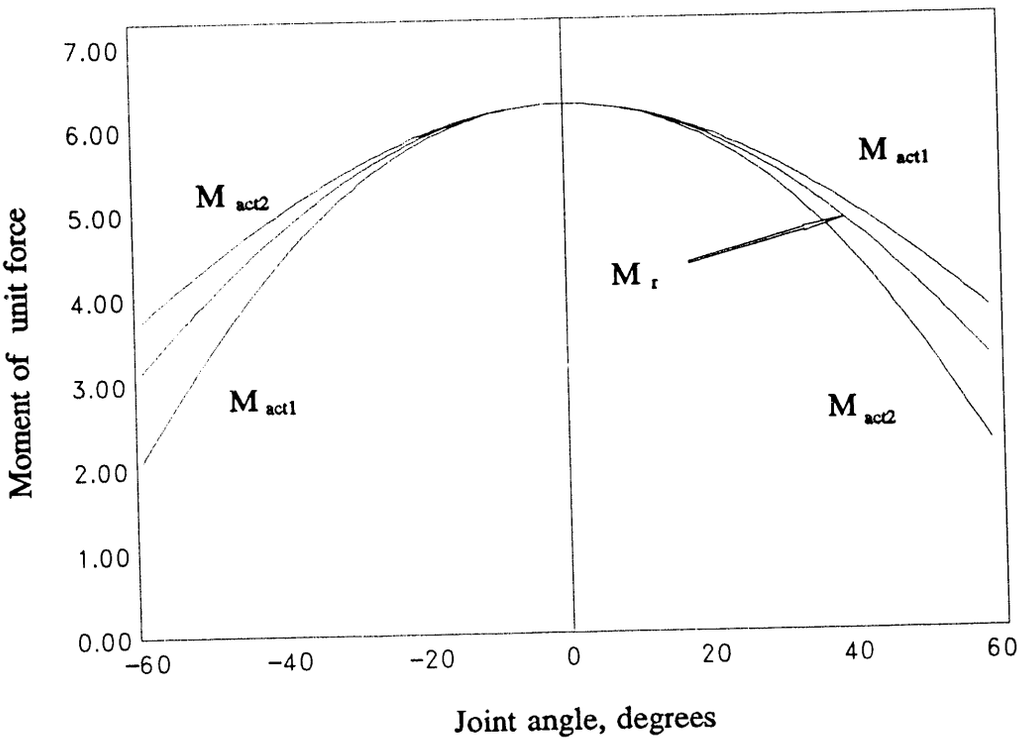

Figure 4.4.2. Joint torque as a function of theta.

Acceleration and deceleration impose other load requirements. It is assumed that high speed and accelerations will not be necessary or even desirable in vertical navigation. Joint torques in the horizontal plane arise from inertial affects and from rolling or sliding friction of the wheels. These loads are much smaller than the quasistatic loads from vertical navigation. The parallel planar actuator's mechanical advantage closely matches expected driving loads. This makes the mechanism well suited for the application.

These relationships allow for the sizing of the linear actuators. The loads the actuators see are the same ones the structure or skeleton of the ATMS sees. The parallel

planar actuators has one non-actuated prismatic joint and five non-actuated revolutes. Each must be designed to withstand the expected loads.

Another concern in the design of the mechanism is collision of components. Collision of components native to a segment and collision between components of different segments is considered.

Design objectives for the parallel planar actuated joint design are driven by the requirements placed on it by its operational environment. General objectives are range of motion, minimization of weight, and load carrying capacity. These objectives are coupled.

In order to evaluate the suitability of the parallel planar joint actuation scheme for the ATMS, it was decided to design and fabricate a working model. The first step was to design a segment and the mechanics of a single two degree of freedom actuator. The second step in this evaluation is the fabrication of a four degree of freedom segment. Performance evaluation is performed for each step. Controllability under load is of prime concern. Secondary is evaluation of the structural integrity of the design.

The mechanical design, fabrication and testing of step one has been performed. A test stand was designed that allowed the body with a two degree of freedom parallel planar actuator to be tested. Loads were applied that duplicate expected loads for a segment of an ATMS undergoing vertical or bridge navigation. The mechanism meets controllability criteria. It is weak on minimizing weight and in stiffness normal to the plane of the parallel actuator. Because of this, redesign of the mechanism is ongoing. A change of materials from aluminum to a composite is being performed. Redesign of the non-actuated prismatic joint is being performed.

4.5 MECHANICAL DESIGN:

The mechanical design will be presented in the form of mechanical drawings. Actuator selection will be covered, along with feedback schemes. The basic apparatus designed and fabricated to test the parallel planar actuation concept is illustrated in figure 4.5.1. Each of the mechanical subassemblies are detailed and a brief description is given. Mechanical drawings relative to each subassembly are referenced by their parts names. The drawings can be found in an attached appendix.

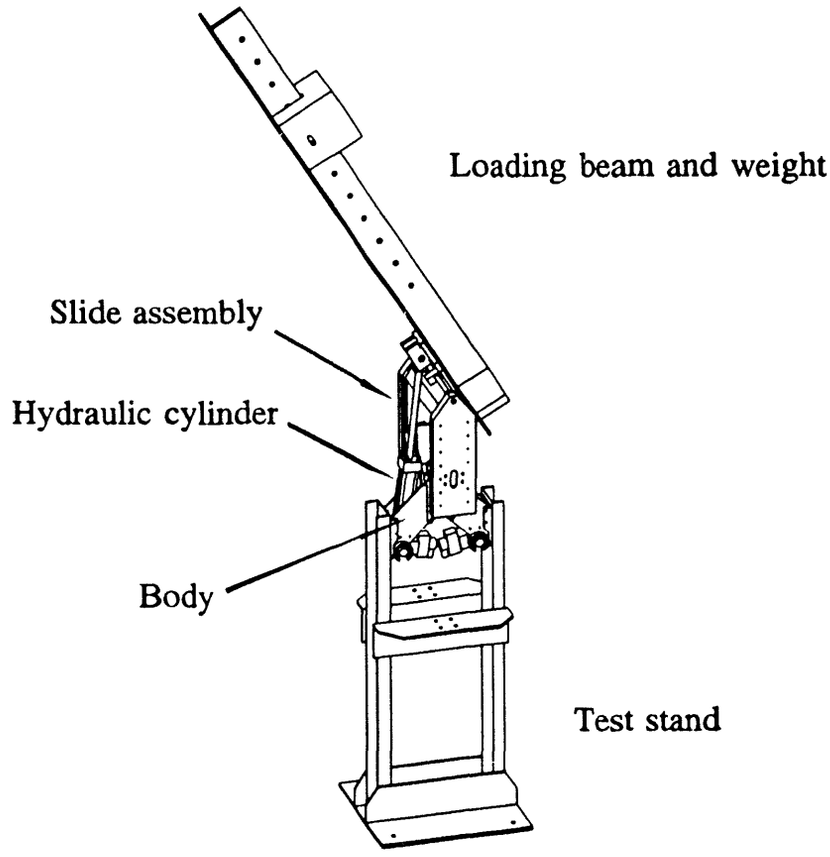

Figure 4.5.1 ATMS test stand.

Test stand Parts:

Loading beam	stand
Weight block	base
Beam	legs
	angle braces
	gussets

The test stand was fabricated from cold rolled carbon steel shapes. It's principle function is to apply a joint load that can be varied. The loading arm has a sliding weight for applying moments to the actuator. The test stand holds the body. The body is illustrated in figure 4.5.2.

Body parts:

Caps	Webs	Bearings
cap1	web	bearing ring
cap2_1		bearing block
cap2_2		bearing liner
		bearing cap

Hydraulic cylinders: Airdro MY-MT2 2 in bore X 10 in stroke

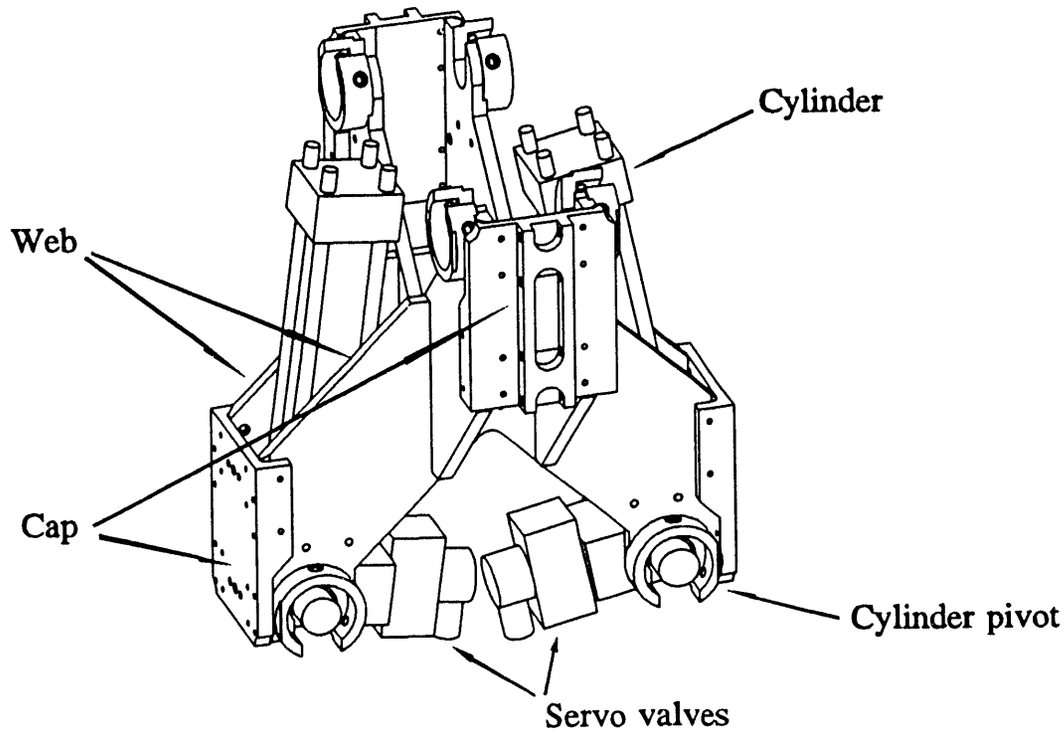

Figure 4.5.2 Version 3 body with 1 pair hydraulic cylinders.

Body:

The material used in the fabrication of the body was 6061 T6 aluminum. The body is constructed of many parts that were welded together. This process produced some heat distortion that had to be corrected. The illustration does not show the bearing rings and bearing caps used to fix the trunions of the cylinders in the body. Recirculating ball bearing blocks are mounted on the caps of the body. Their ground slides are mounted in the slide assembly. The slide assembly is shown in figure 4.5.3.

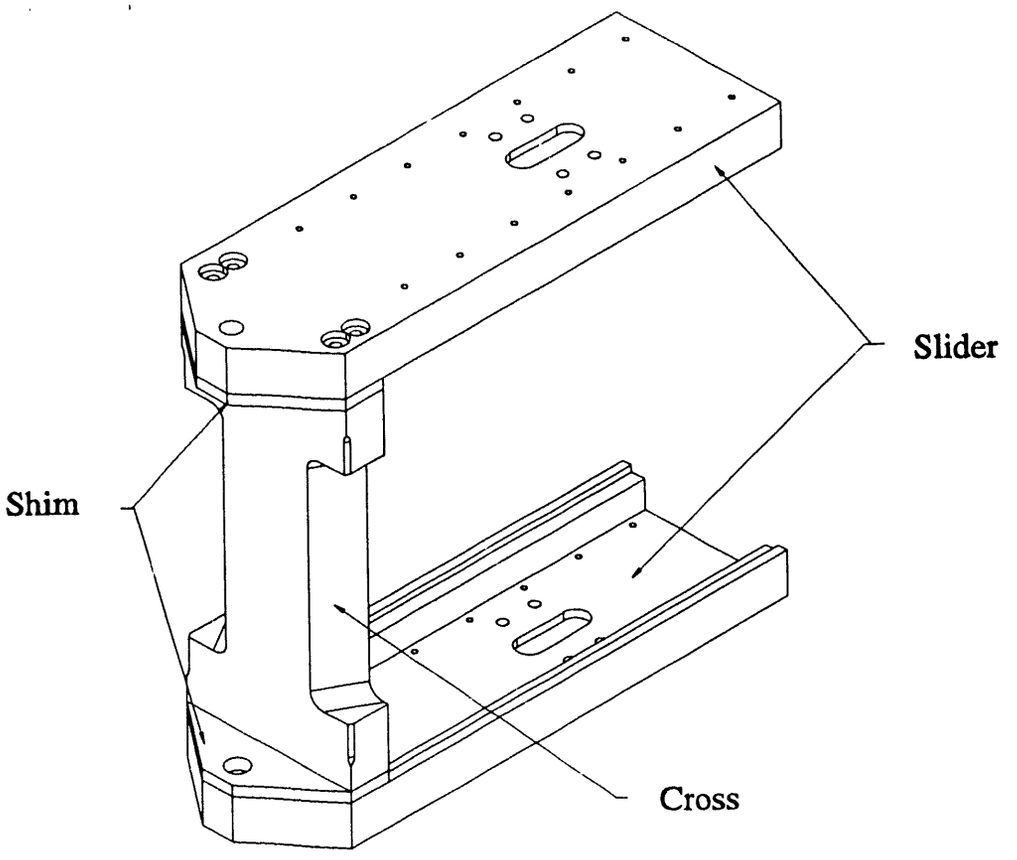

Figure 4.5.3 Slide assembly for version 3 body.

Slide assembly parts:

slider cross shim bushing shaft

recirculating ball slides: THK type HR 2042

Slide Assembly:

The slide assembly was fabricated from 2024 T351 aluminum. There are two sets of recirculating ball bearing slides mounted in the slide assembly.

Actuator selection:

From the previous discussion concerning the mechanical advantage of the mechanism, it can be seen that the moment generated will range from approximately r_1 to $2*r_1$ times the load a linear actuator can produce.

Due to cost and availability, servo hydraulics was chosen to power the first segments. The maximum driven moment is set at 470 N/m. The minimum is 235 N/m. The mechanism can meet bridge navigational requirements for small changes in elevation. This is based on a minimum weight per unit length at 70 N/m.

A two inch bore cylinder with a 1 3/8 inch diameter rod provides enough force to achieve the required moments. This cylinder has an oversized rod because it has an integral linear transducer. This allows feedback of the cylinder length directly.

The passive slide was designed using linear recirculating ball bearings. These bearings run on induction-hardened ground steel raceways. They are purchased off the shelf.

Feedback:

Two methods of determining the configuration of the parallel planar manipulator exist. One is feedback of actuator length and the other is feedback of the slide length and ring angle. The test segment has both types of feedback to allow evaluation of each type. Feedback of cylinder length with an integral LVDT results in a cylinder with an oversized rod (reduced pull force). This type of cylinder is also heavier that a normal servo hydraulic cylinder (by approximately 25%). Linear displacement is measured by LVDT's in both cases.

These are absolute devices with no need of a homing sequence. Angular displacement is measured by an absolute encoder.

4.6 ONGOING DEVELOPMENT:

The weight of the first body/slide/actuator configuration is above criteria, primarily due to excessively heavy actuators and slide. Actuators without LVDT's are considerably lighter than actuators with LVDT's. The second body will utilize the lighter actuators. Slide length will be feed back with an axially mounted LVDT. Joint orientation will be feed back using an absolute encoder.

Further weight reduction will be effected by the shift from aluminum to a composite. Kevlar, graphite, and other reinforcing fibers in polymer matrices are being evaluated. Initial prototyping will most probably be with a hybrid of two fibers in one matrix.

Servo-hydraulic actuators were chosen initially because of availability and experience in the area. Some effort was expended in evaluating electro-mechanical actuators. Further effort in this area of actuation is expected in the future.

Appendix: ATMS mechanical design drawings

ATMS Test Stand

Test stand: stand

Material: structural steel	sfile: ne
	pfile:stand

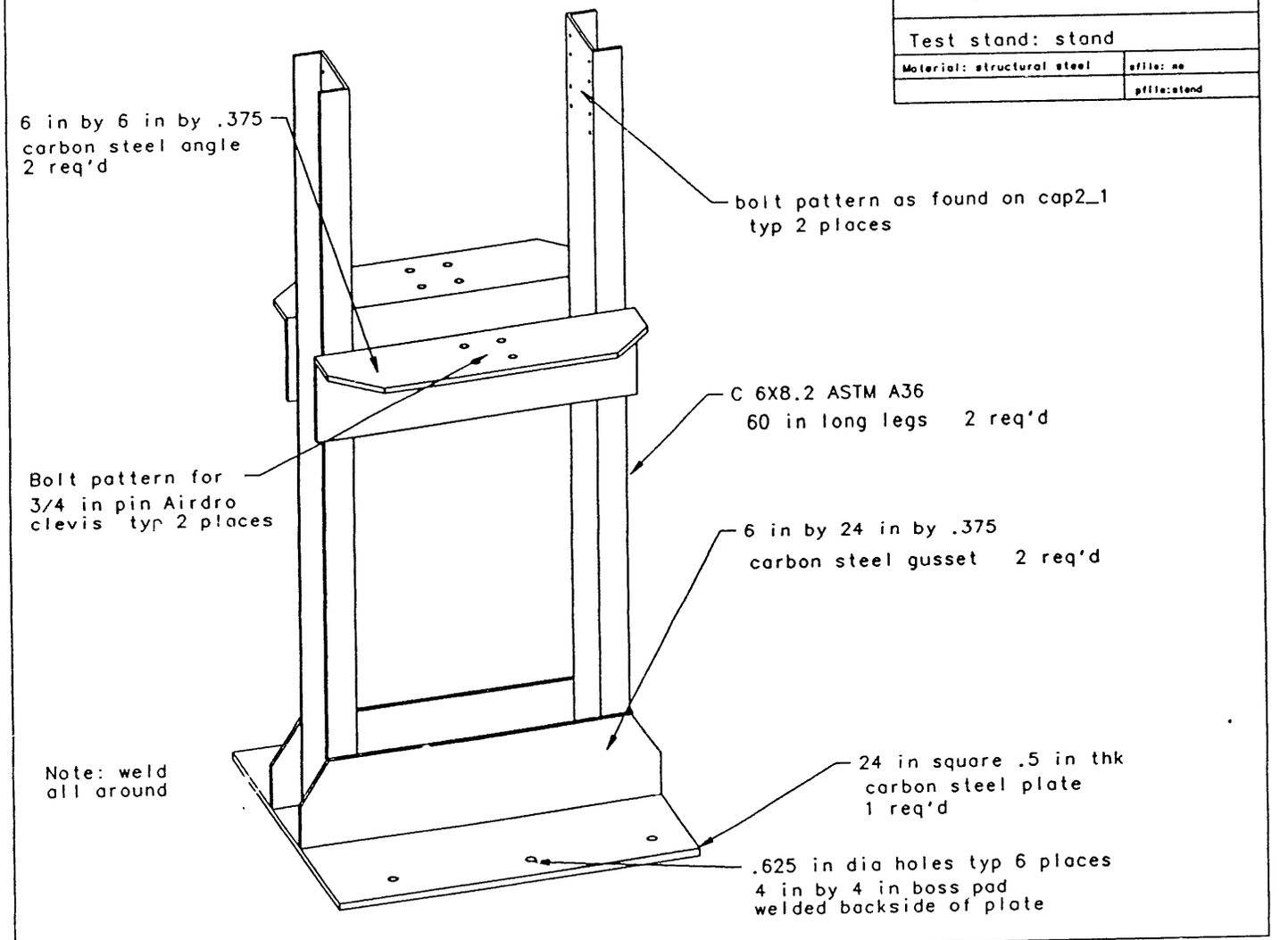

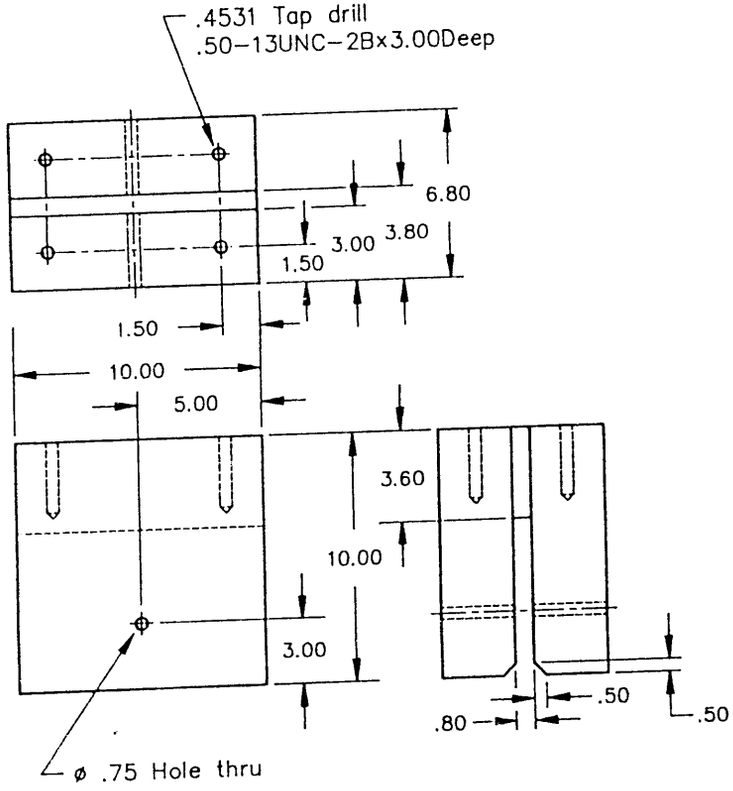

Material: Steel

Note: Use steel plates of any thickness to obtain the required dimensions.

Weld plates together along all seams.

ATMS Proto	
Weight block	SCALE None
John P. Webb	9/2/91

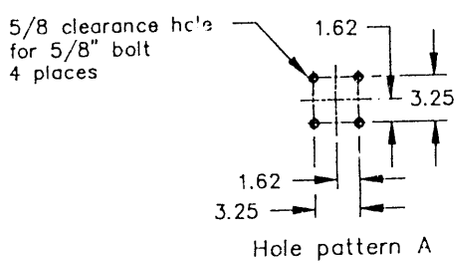

Hole pattern A

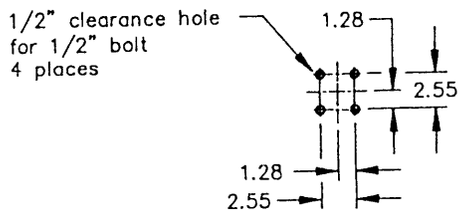

Hole pattern B

Material: 6" x 6" x 3/8" Steel angle

Note: Weld angles together along all seams before drilling .50" holes.

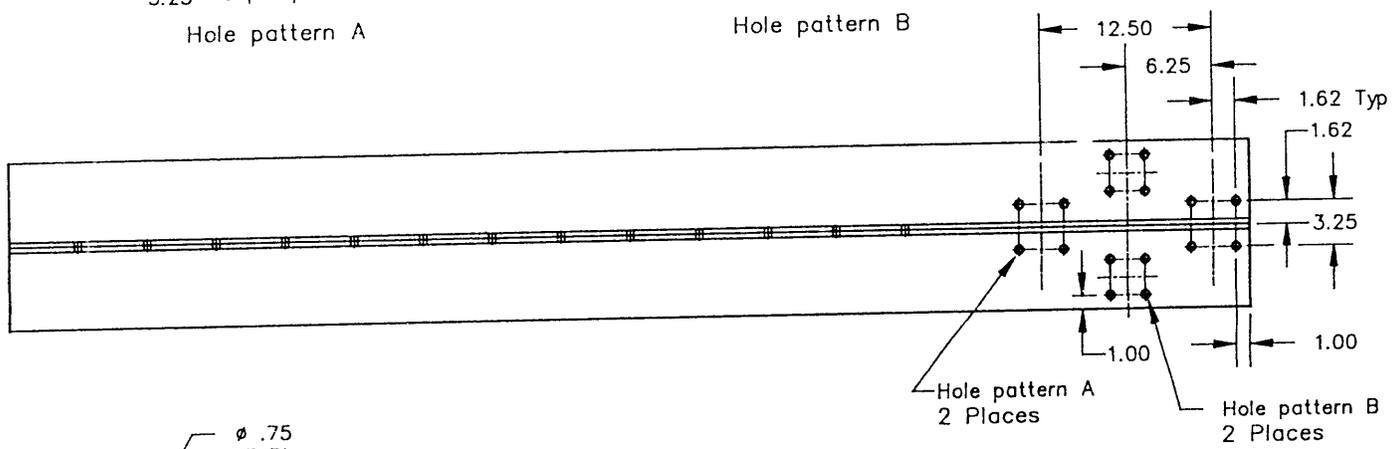

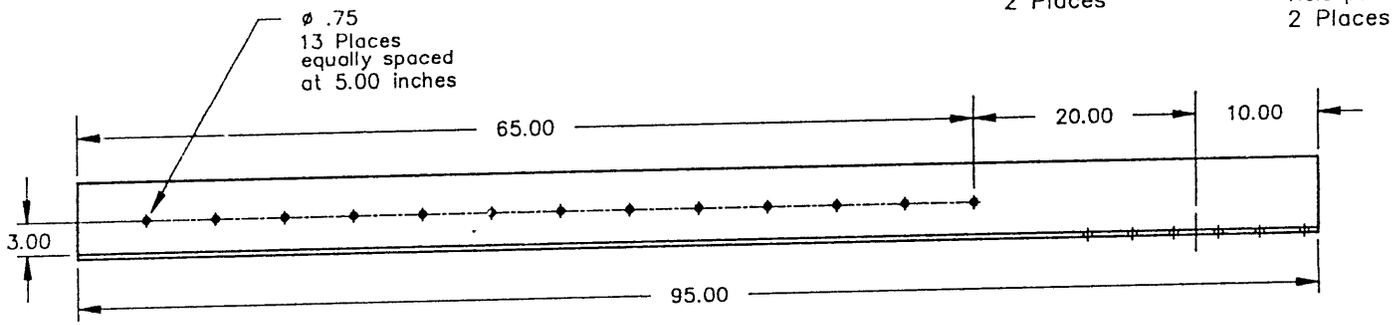

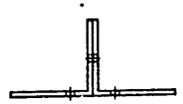

ATMS Proto	
Beam	SCALE None
John P. Webb	9/2/91

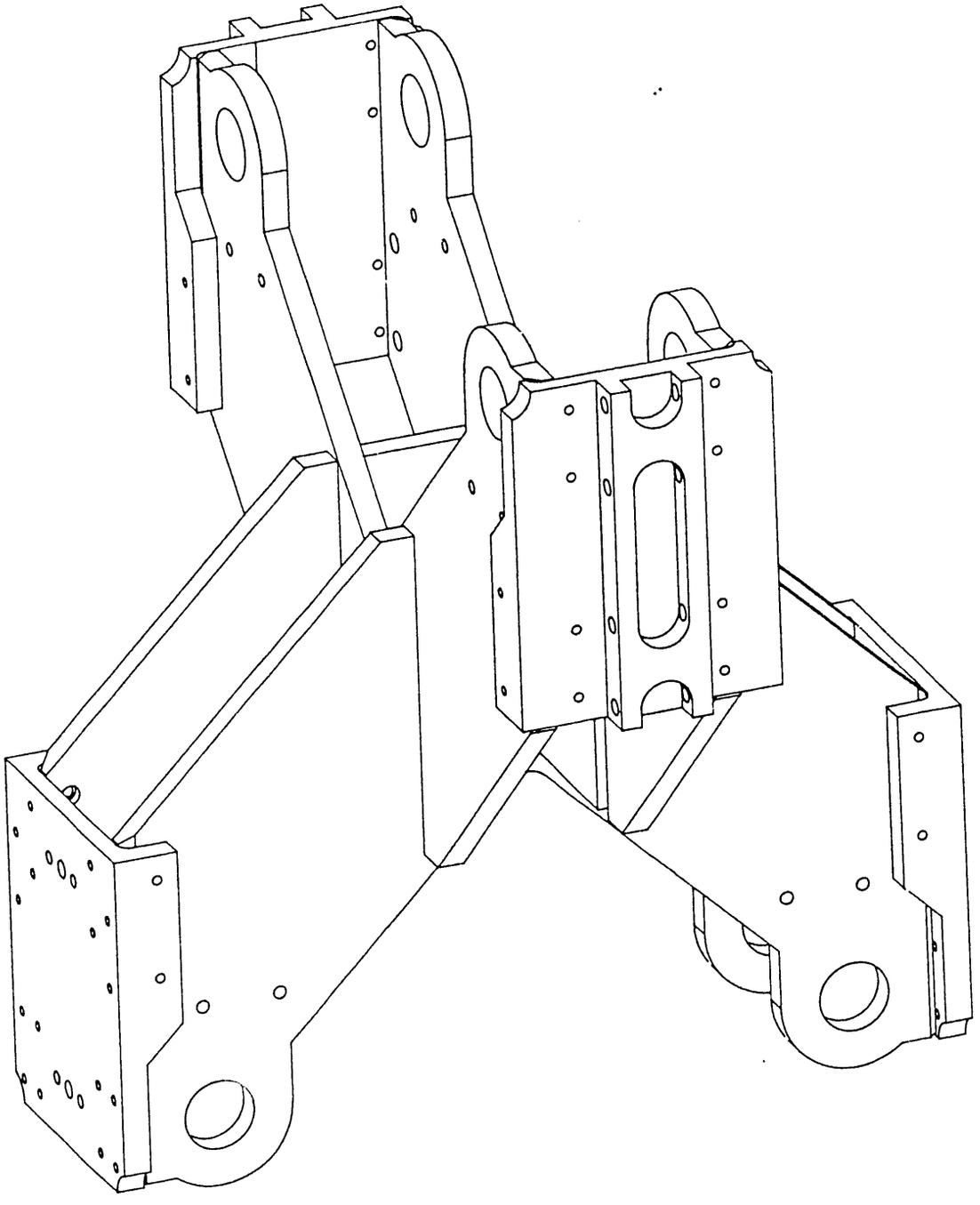

ATMS Body Structure

Version 3

ATMS Test Stand

Base:Pact2 Assembly det

Material: 6061 t6 Al | sf:b3

pf:pact2_rc

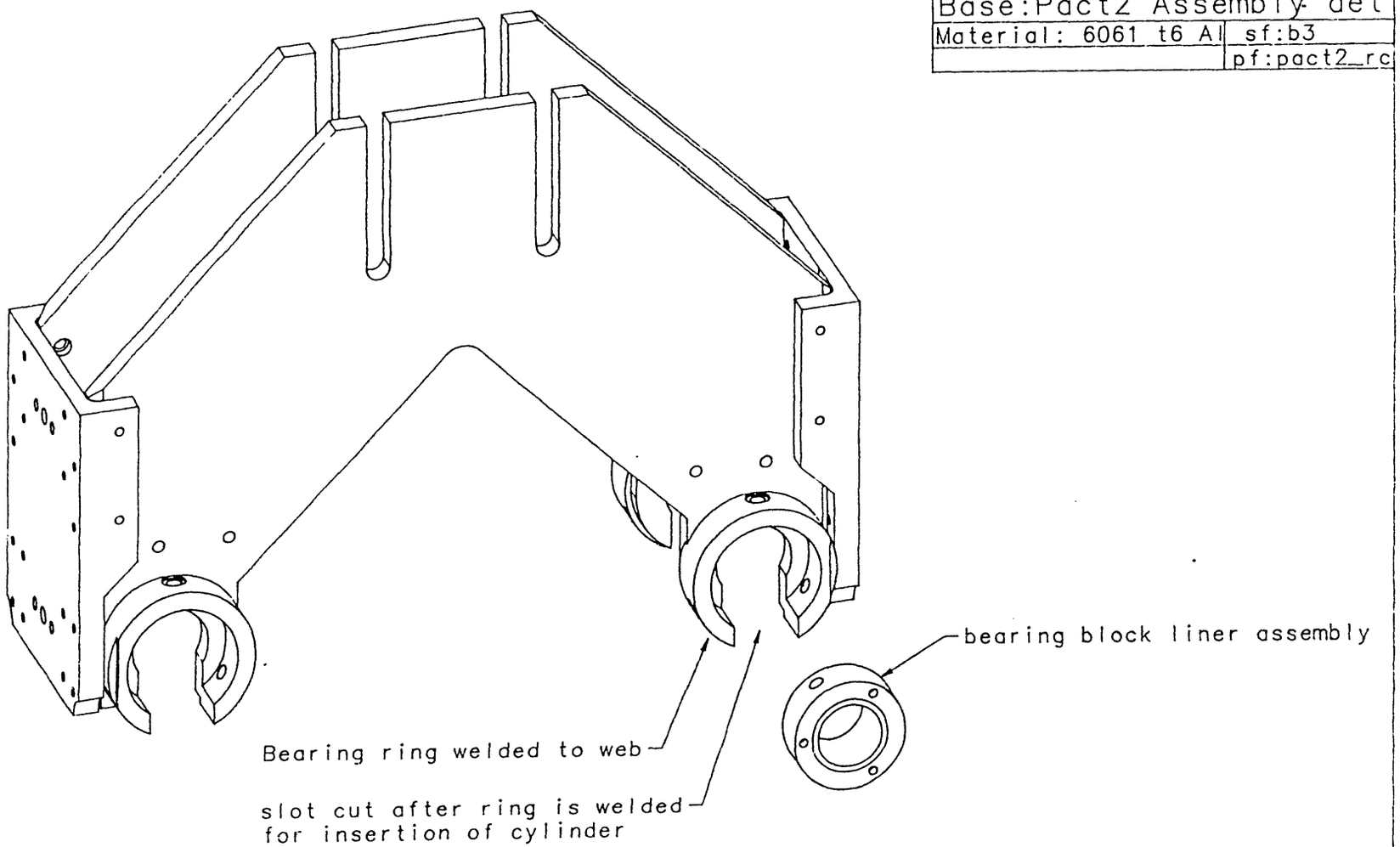

ATMS Test Stand

Base:Web isometric

Material: 6061 T6 Al.	sf:b3
	pf:webiso

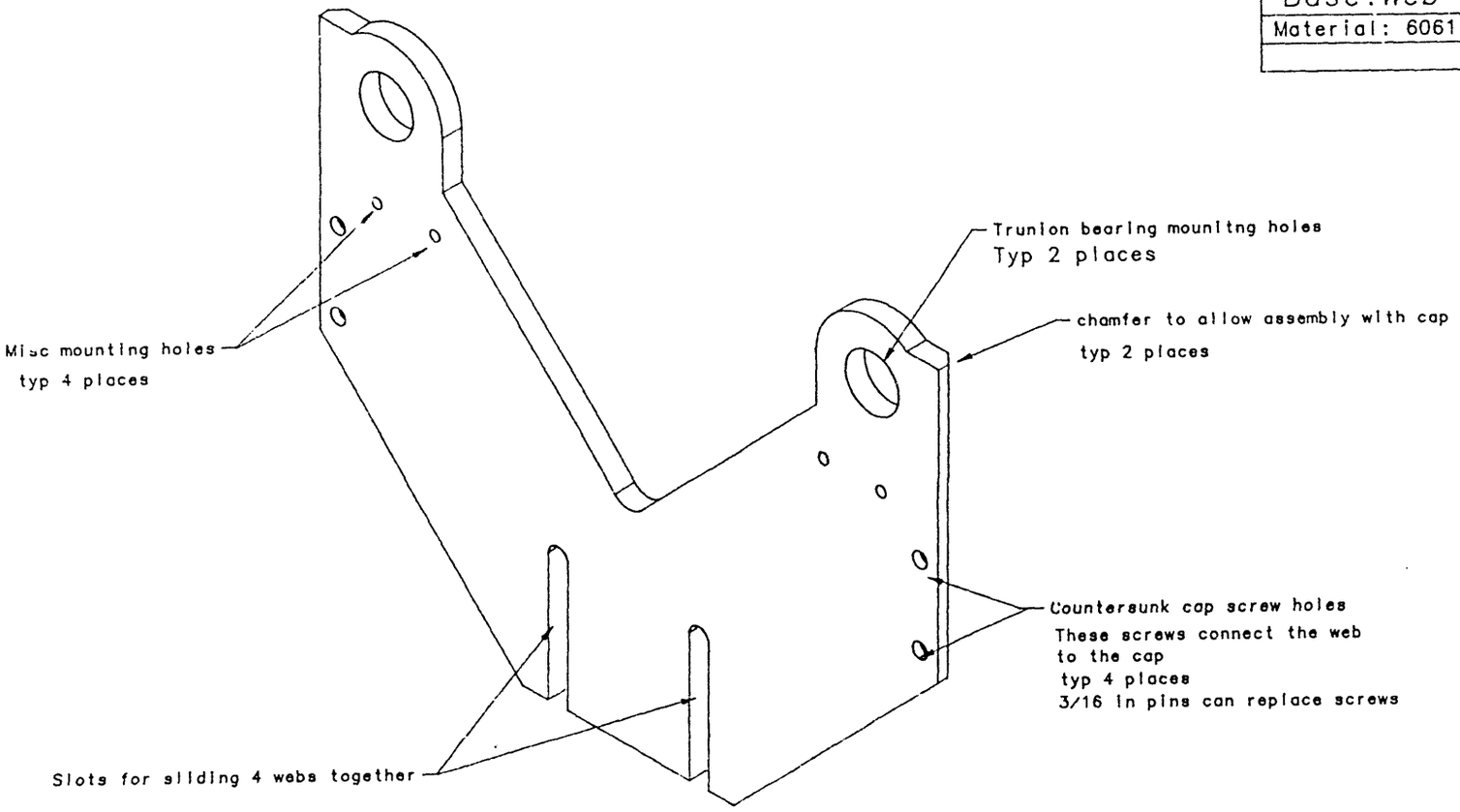

Construct out of 1/2 in thick
6061 T6 Al. plate

ATMS Test Stand

Base:Web 4 required

Material: 6061 T6 Al.	sf:b3
	pf:web

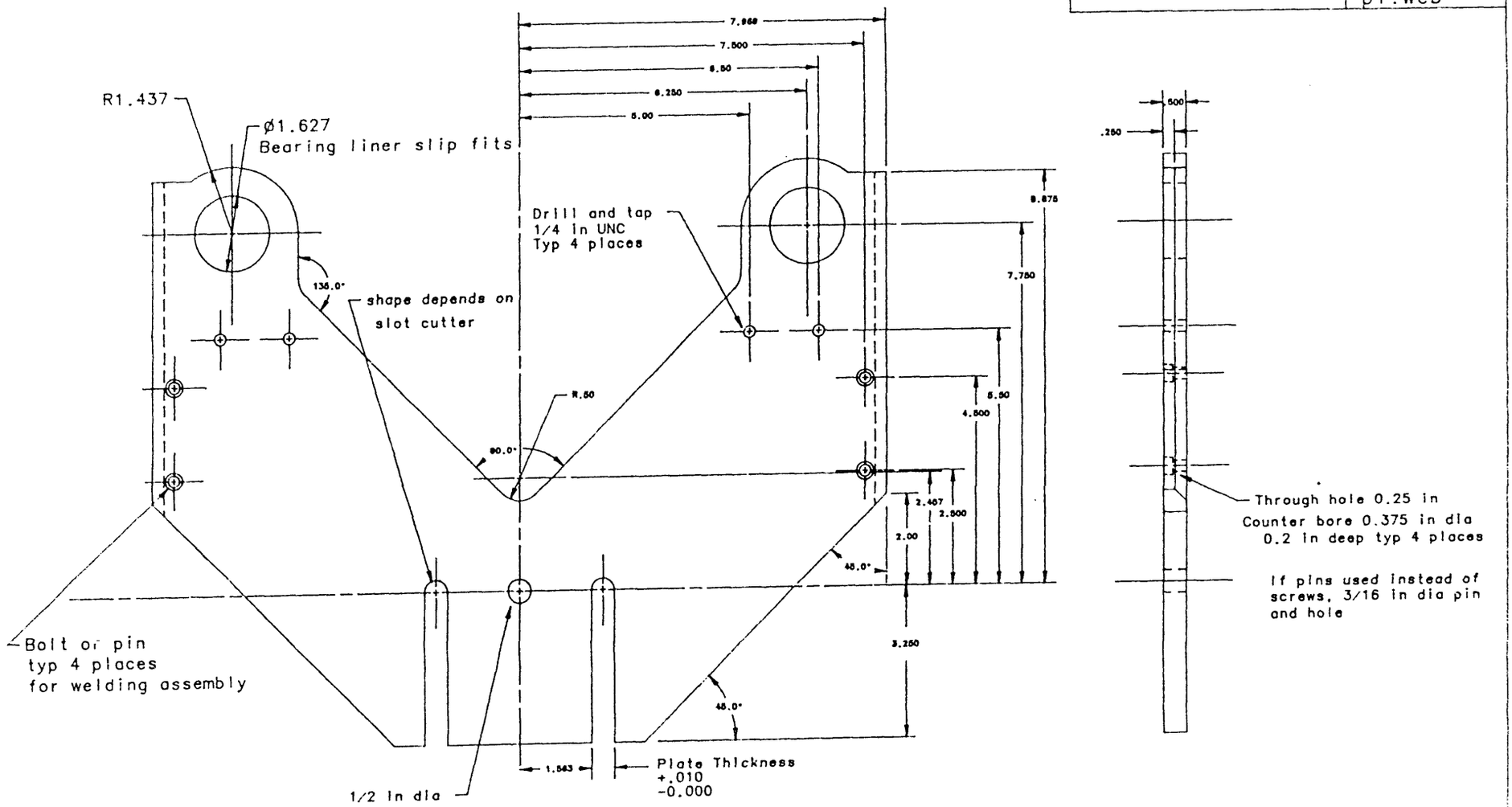

ATMS Test Stand

Base:cap1 isometric

Material: 6061 t6 Al.	sf:b3
	pf:cap1iso

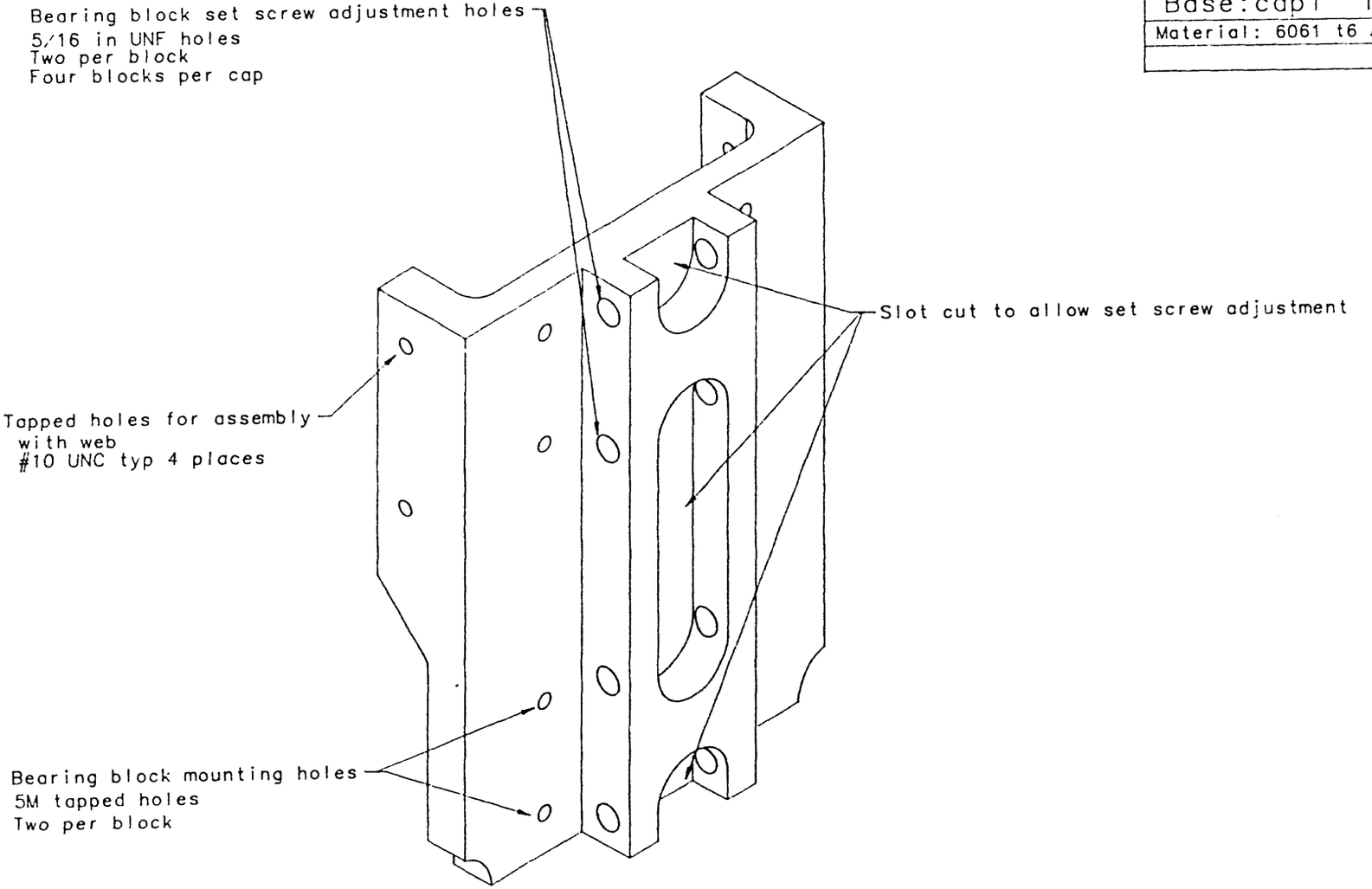

ATMS Test Stand

Base:cap1 2 reqired

Material: 6061 T6 Al.	sf:b3
	pf:cap1

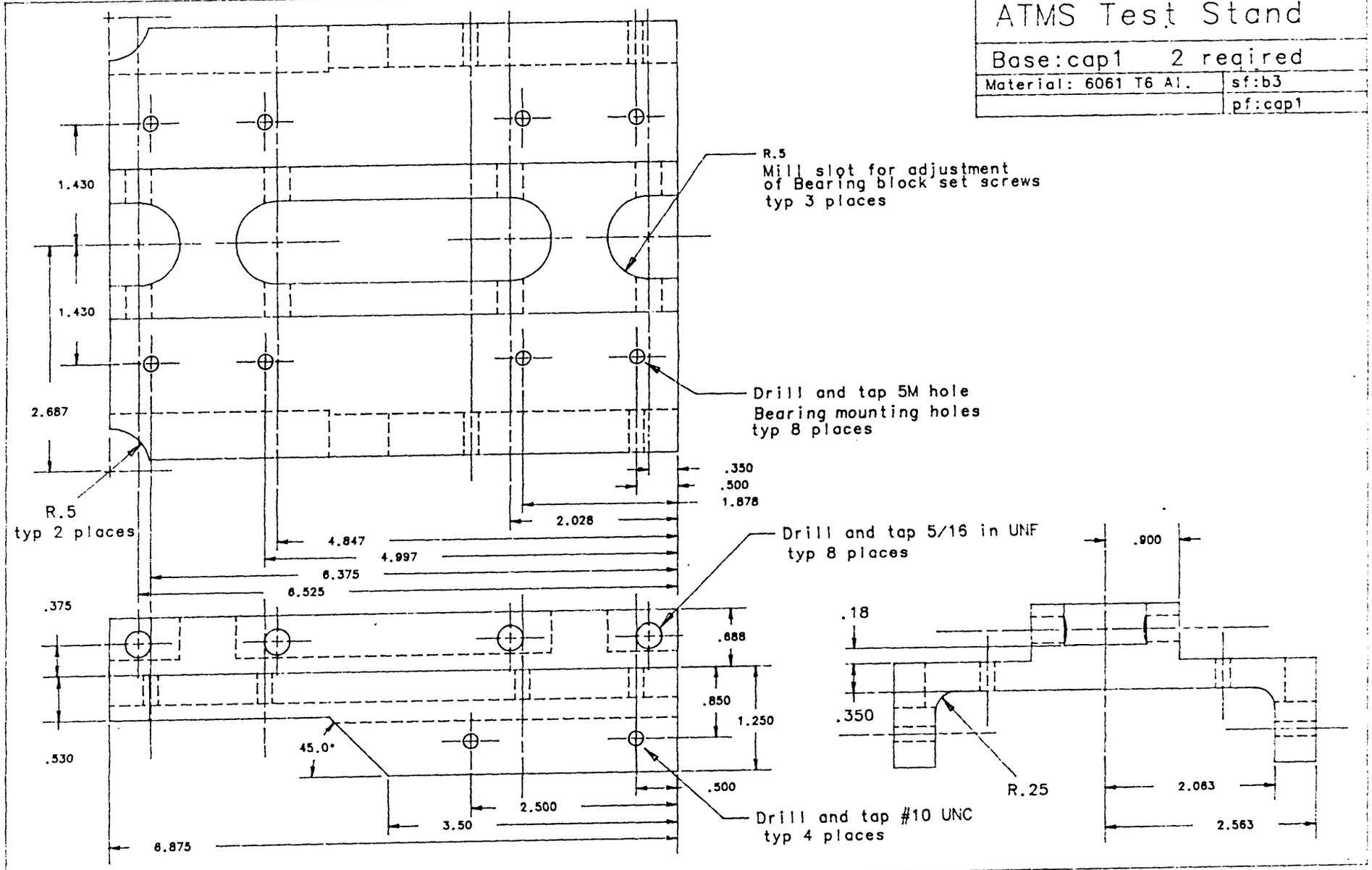

ATMS Test Stand

Base:cap2 isometric

Material: 6061 t6 Al.	sf:b3
	pf:cap2iso

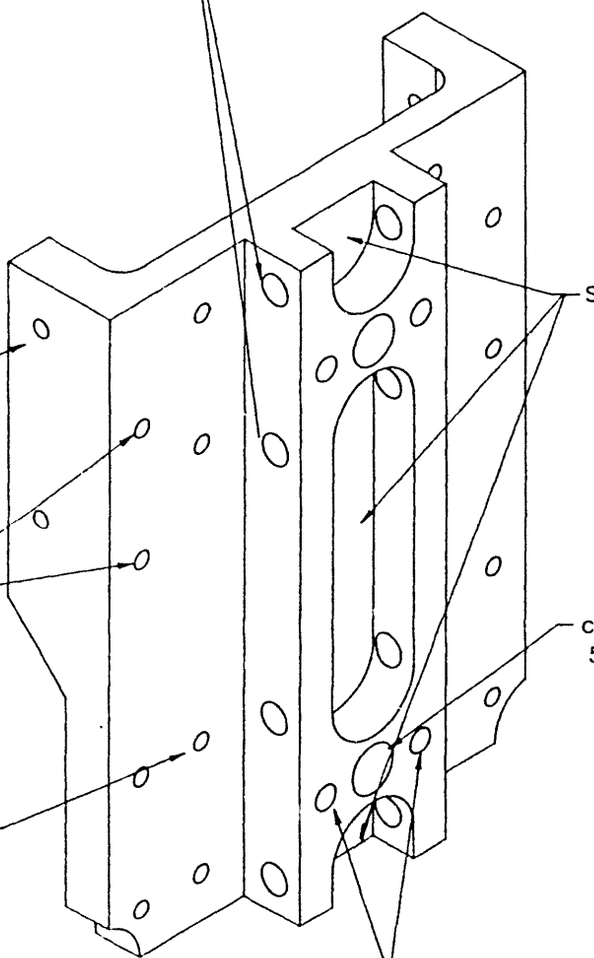

Bearing block set screw adjustment holes
5/16 in UNF holes
Two per block
Four blocks per cap

Slot cut to allow set screw adjustment

Tapped holes for
assemby with web
#10 UNC typ 4 places

bolt pattern for
mounting body in
test stand
8 holes

countersunk cap screw typ 2 places
5/16 in UNC screw

Bearing block mounting holes
5M tapped holes
Two per block

pins 4 places
1/4 in dia

Note: Cap 2 is similar to cap1
It is different in that it is
assembled from 2 parts.
Dimentions of extra holes are
on the parts drawings for cap2

ATMS Test Stand

Base:cap2_1 2 reqired

Material: 6061 t6 Al.	sf:b3
	pf:cap2_1

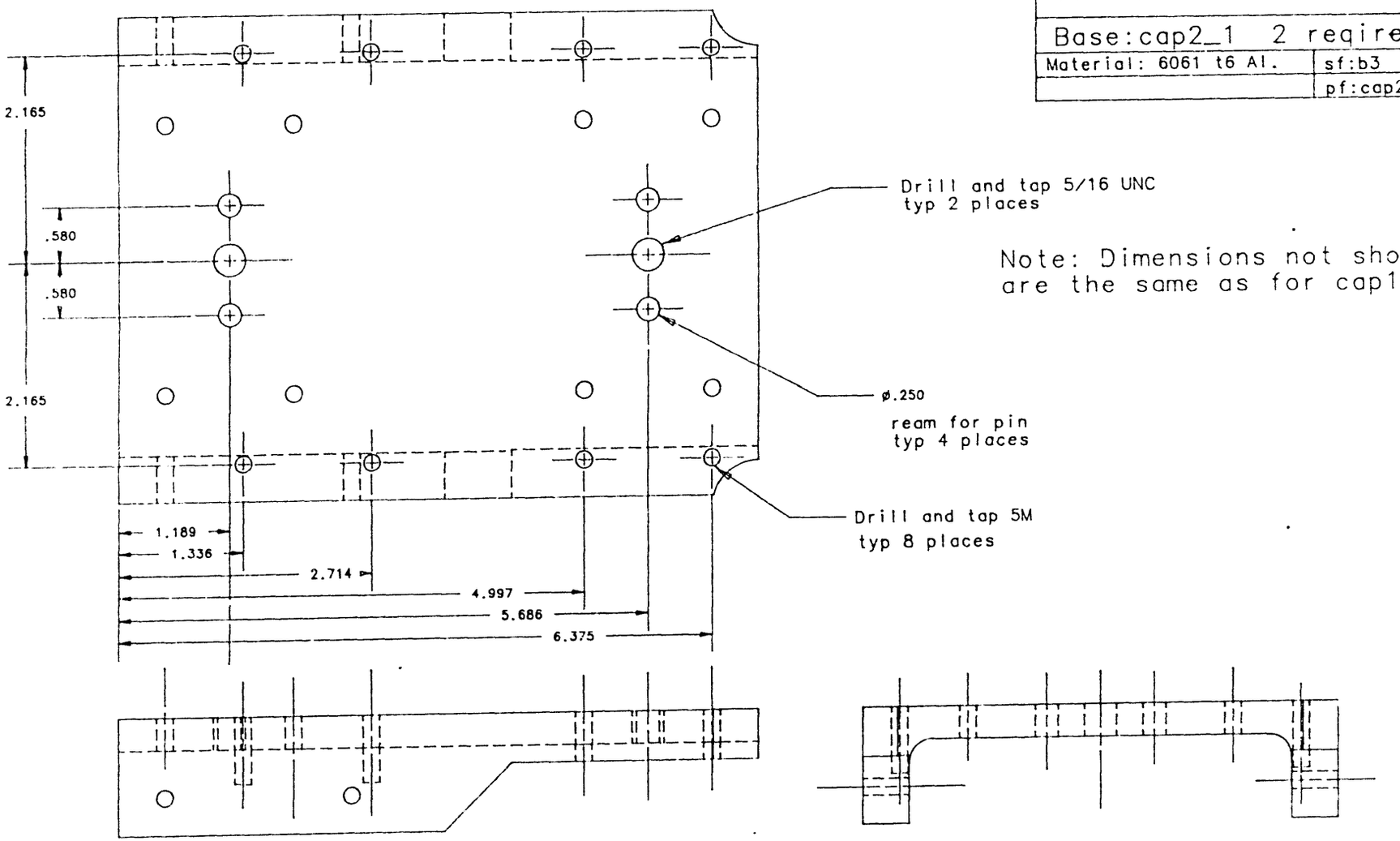

Note: Dimensions not shown are the same as for cap1

ATMS Test Stand	
Base:cap2_2 2 reqired	
Material: 6061 t6 Al.	sf:b3
	pf:cap2_2

Note: Dimensions not shown are the same as for cap1

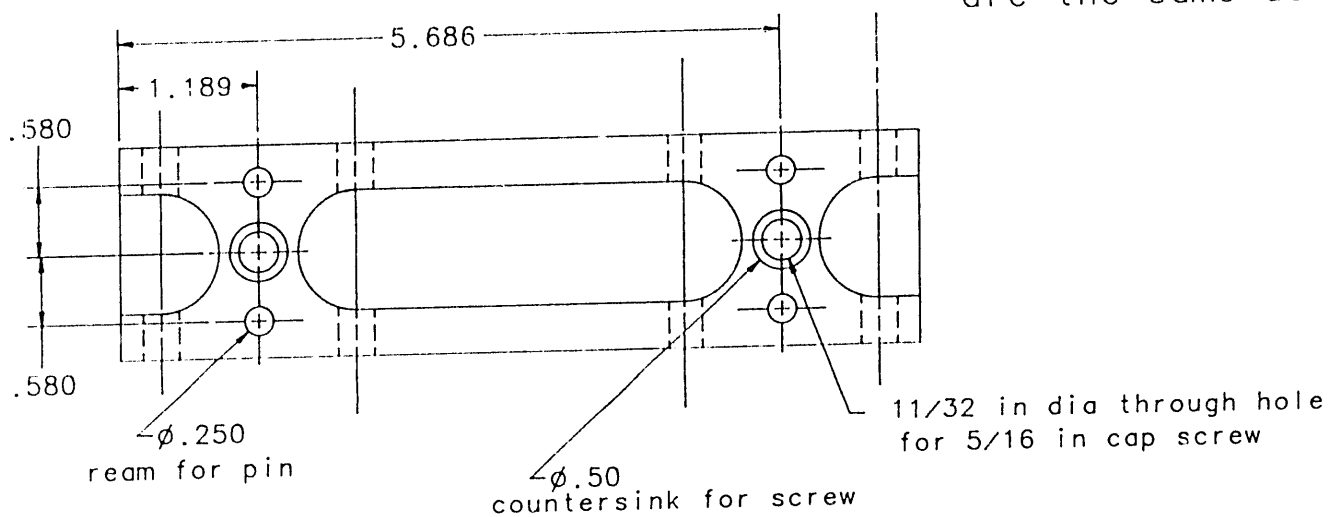

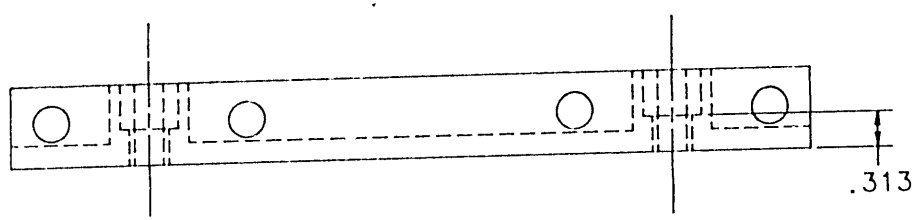

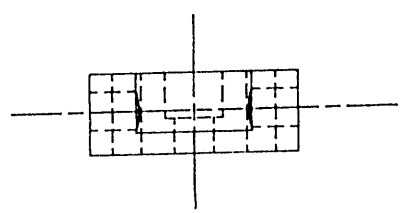

ATMS Test Stand

Base:bearing parts

material: as noted	sf:b2
	pf:bearingp2

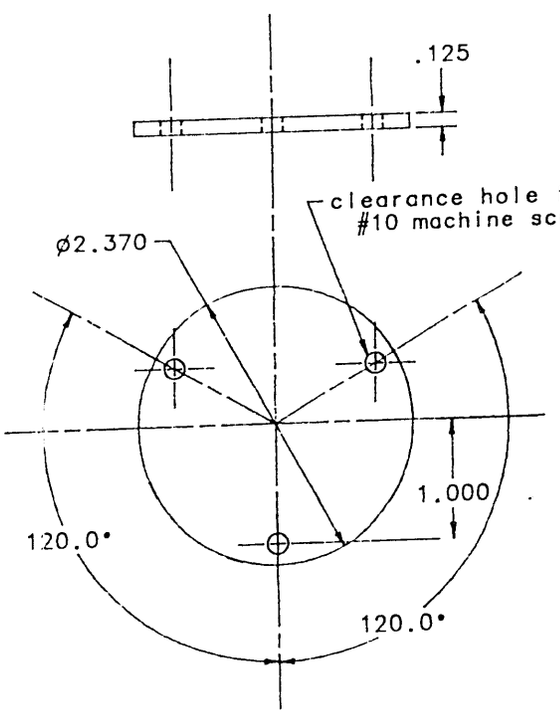

Bearing block cap 8 req'd
material: 6061 T6 al

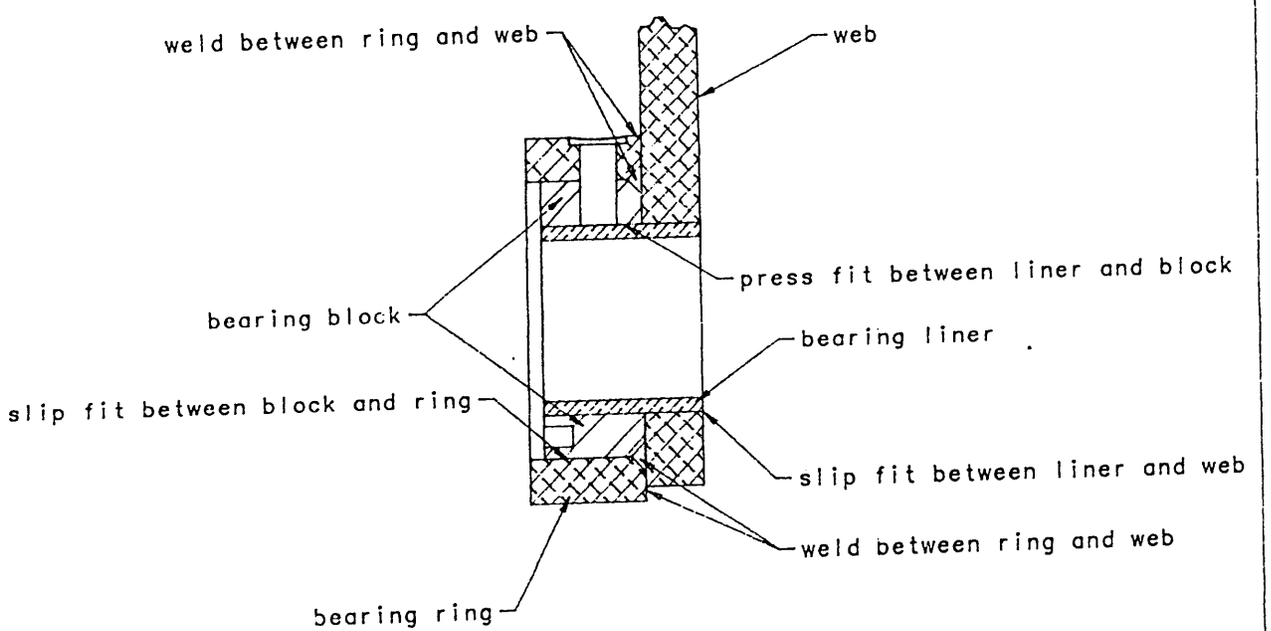

Bearing assembly section

ATMS Test Stand

Base:bearing parts

material: as noted	sf:b3
	pf:bearingp

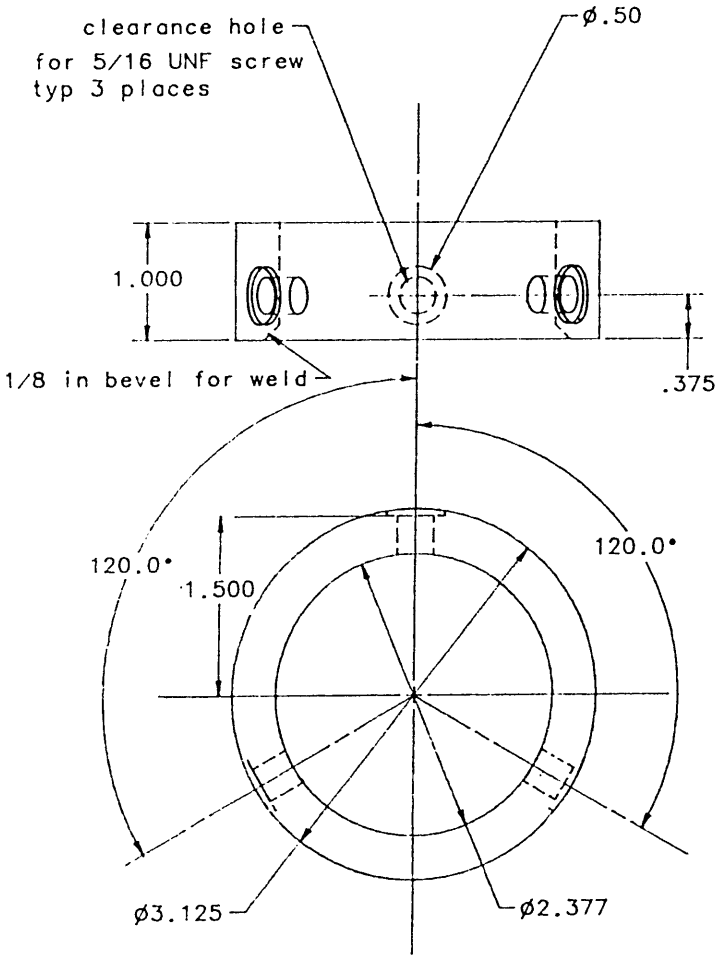

Bearing ring 8 req'd
material: 6061 T6 al

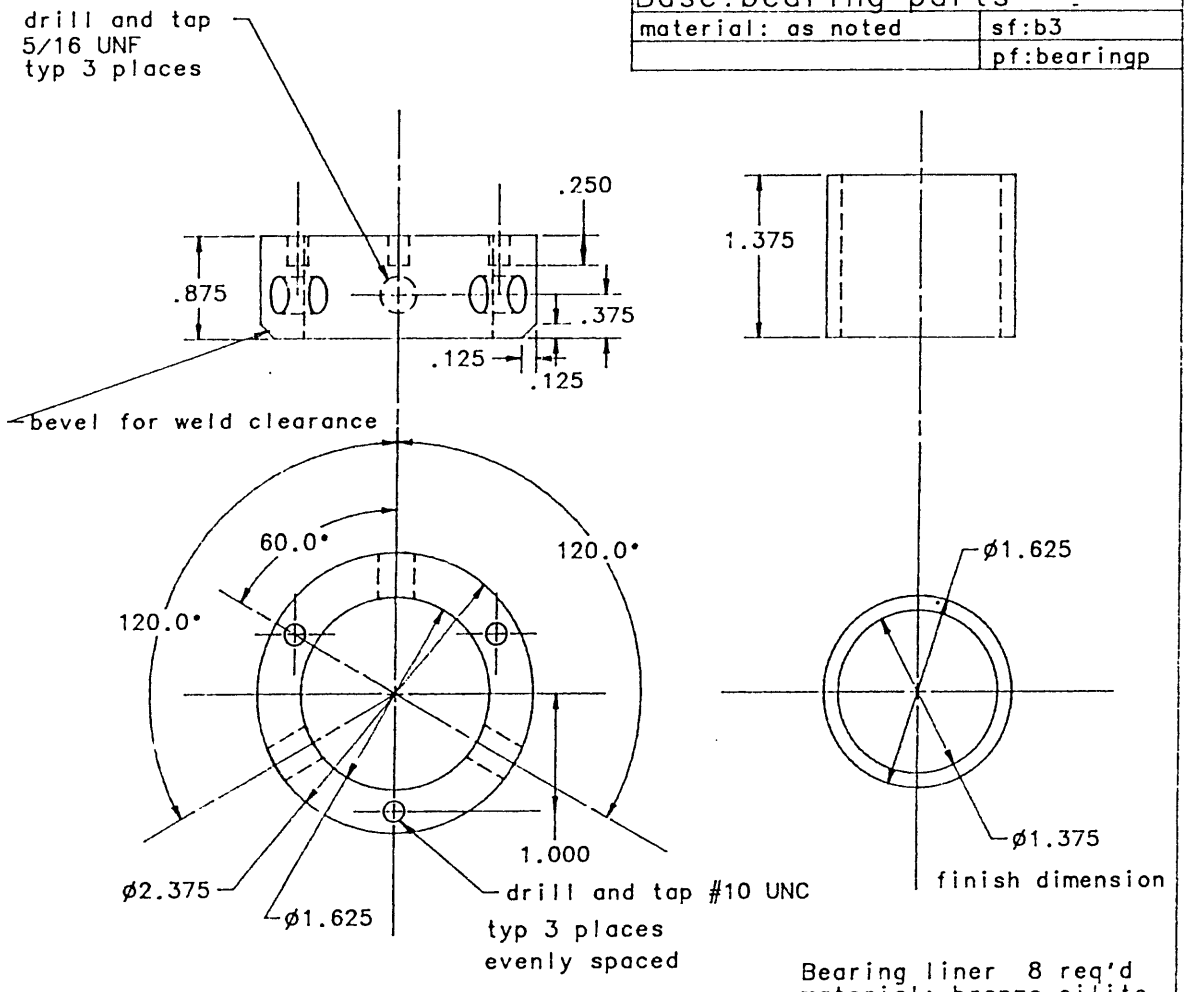

Bearing block 8 req'd
material: cold rolled steel
Block slip fits in ring

Bearing liner 8 req'd
material: bronze oilite

liner is press fit in block

ATMS Test Stand

Slide assembly

Material: 2024 t351 Al	sf:s2
	pf:slideass

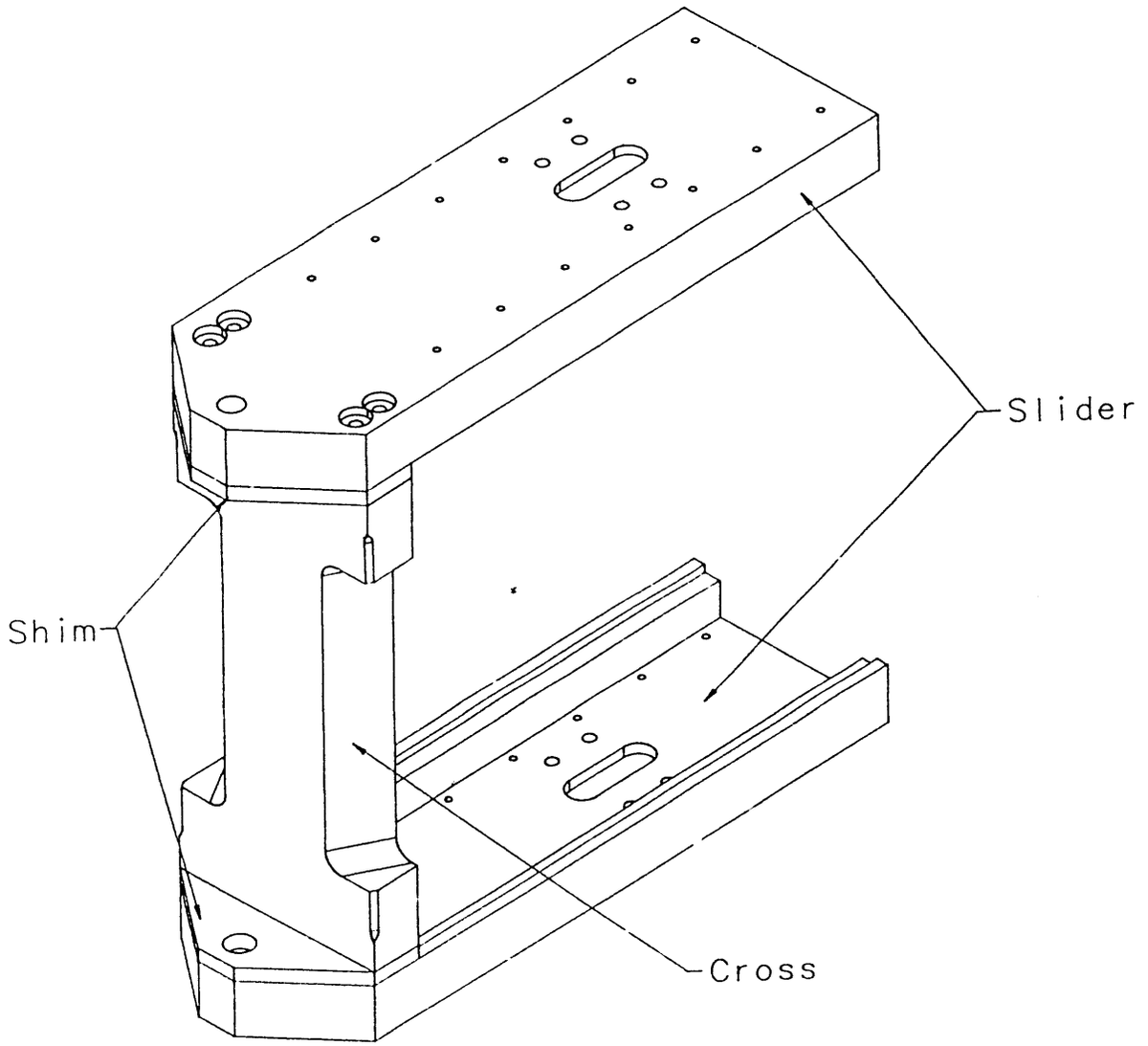

ATMS Test Stand

Slide:slider 2 reqd

Material: 2024 t351 Al | sfile:s2 | pfile:slider2

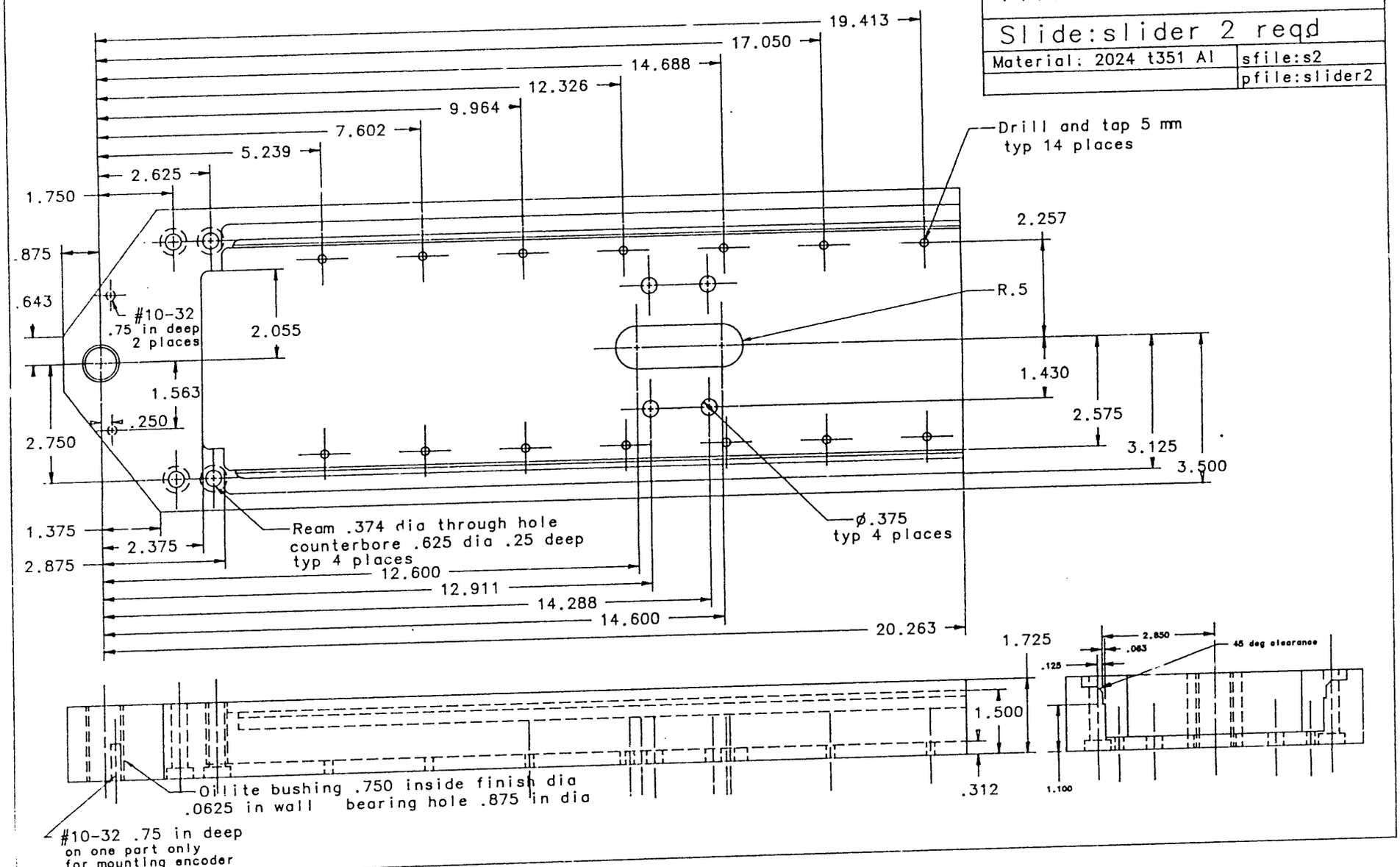

ATMS Test Stand

Slide:shim/bushing

Material: as noted	sf:s2
	pf:shimb

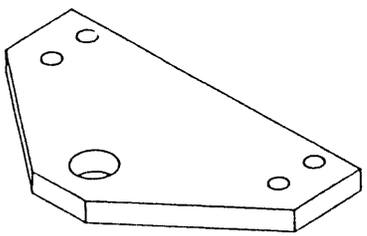

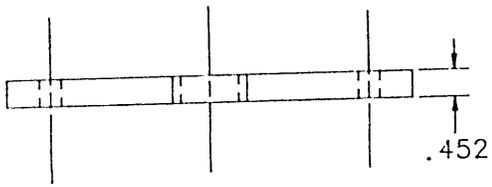

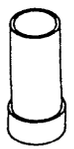

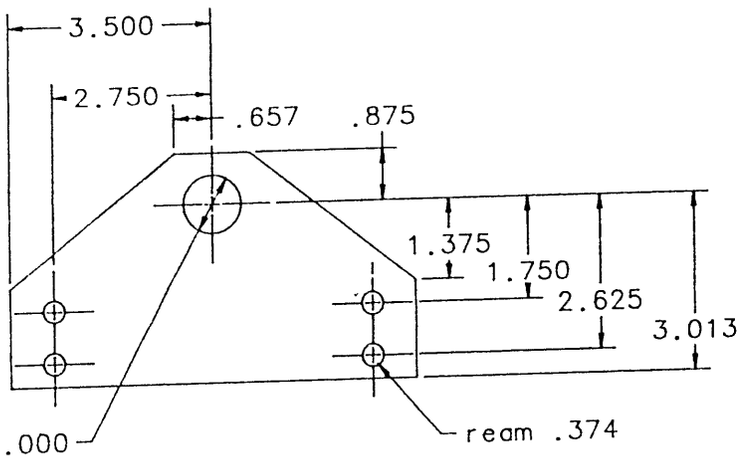

slip fit with bushing

Shim plate material: al 2024 t351 2 reqd

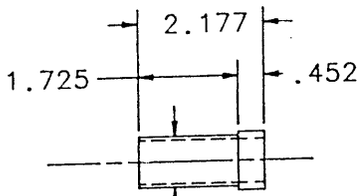

Bushing material: oilite 2 reqd

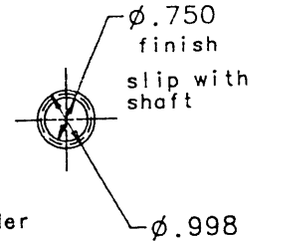

slip with shim

ATMS Test Stand

Slide:shaft/misc

Material: as noted	sfile:s2
	pfile:shafte

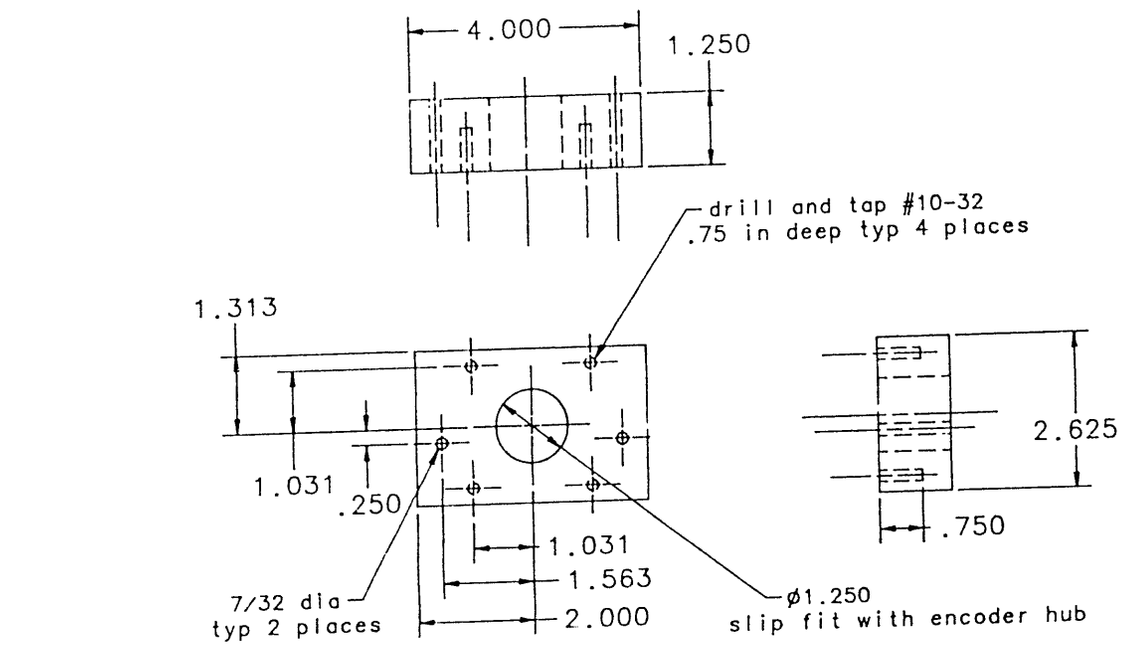

Encoder mount
material: al
1 reqd

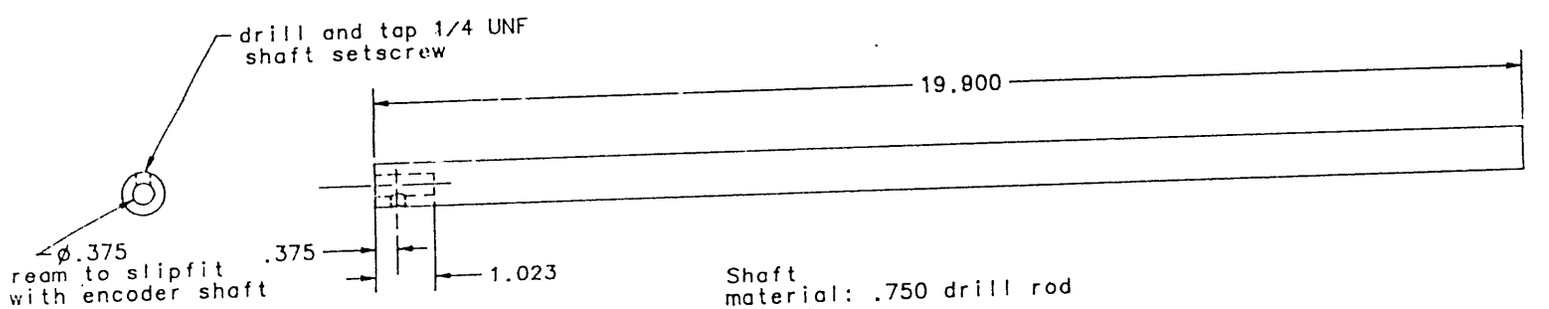

Shaft
material: .750 drill rod
1 reqd

ATMS Test Stand

Slide:cross isometric

Material: 2024 t351 Al | sf:s2 | pf:crossiso

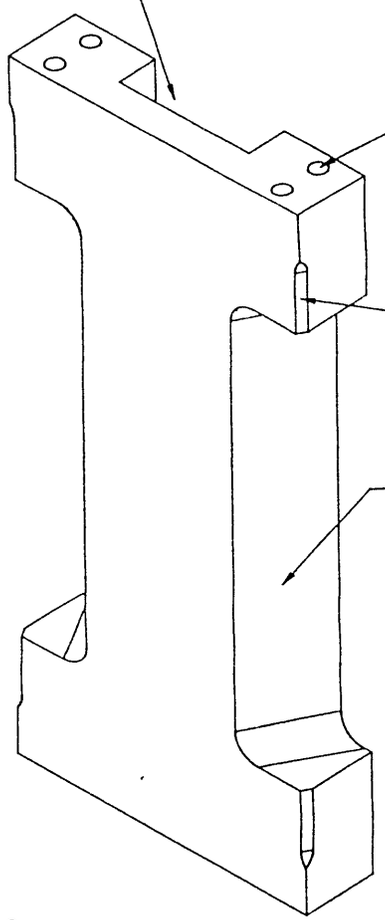

Slide: Cross

ATMS Test Stand

Slide:cross 1 reqd

Material: 2024 t351 Al	sf:s2
	pf:cross

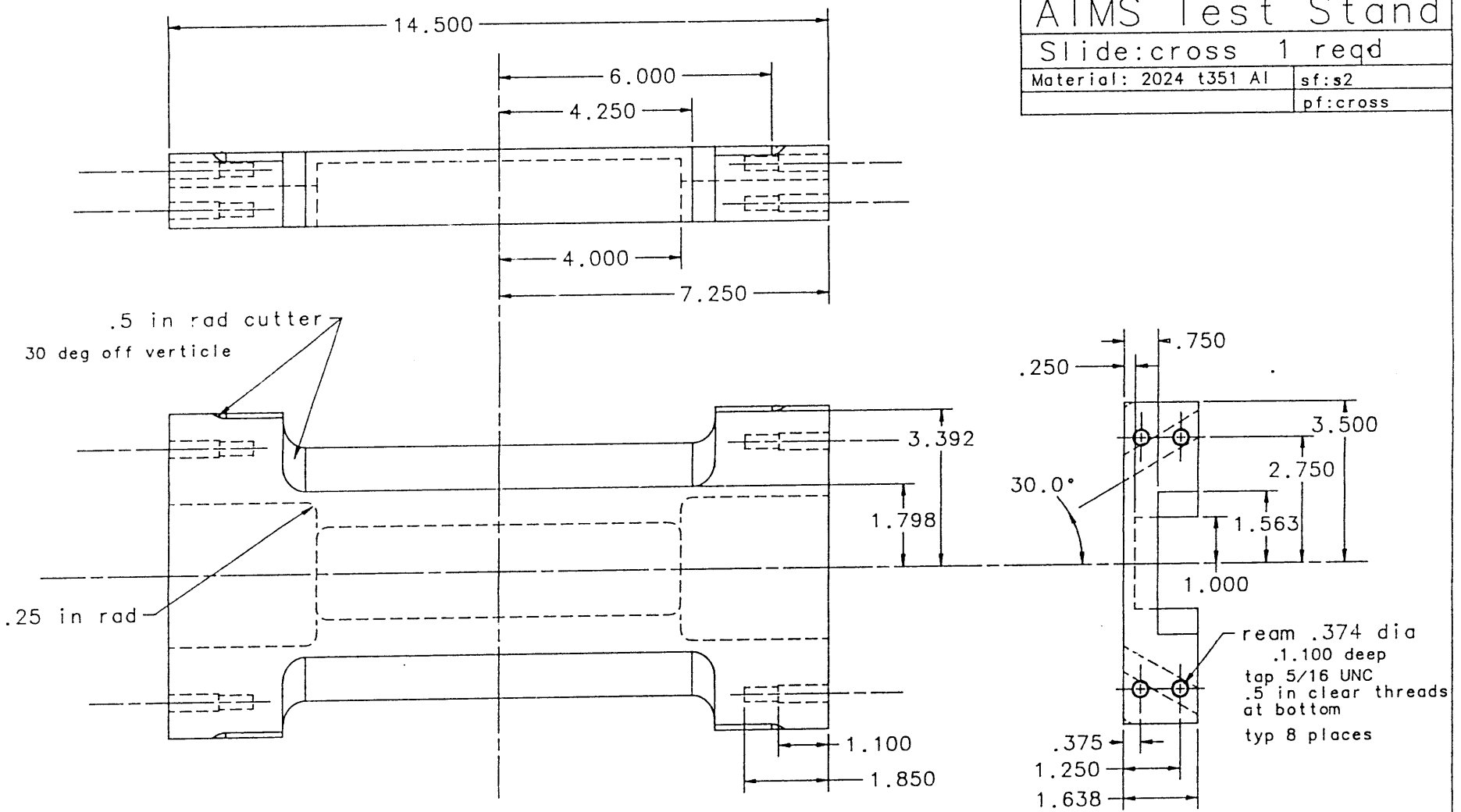

ATMS Test Stand

Misc parts

Material: as noted	sf:s2
	pf:misc1

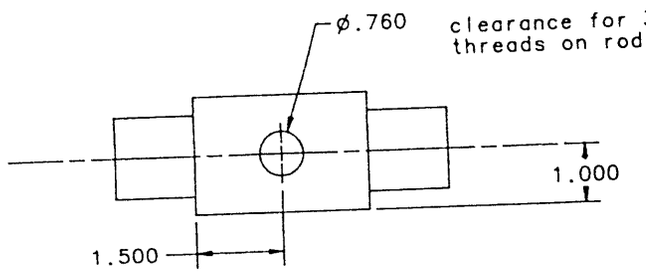

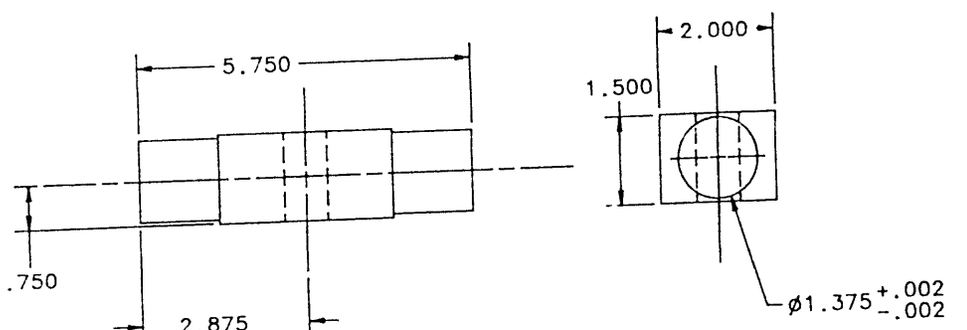

Trunion block
Material: steel
2 reqd

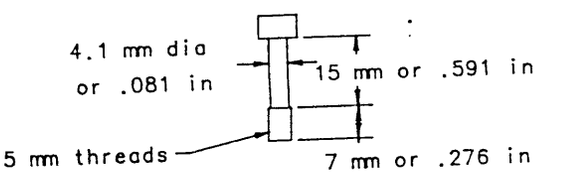

Bearing block Hex socket head cap screw
28 reqd
shank is turned down

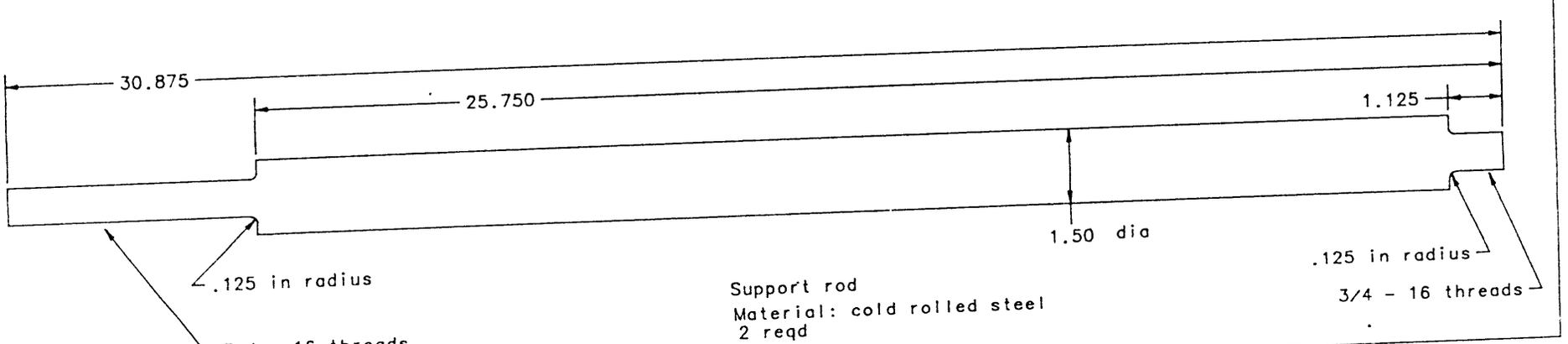

Support rod
Material: cold rolled steel
2 reqd

Computer Software Development and Hardware for the Articulated Transporter/Manipulator System

This section describes the computer software developed and the hardware utilized to control the Articulated Transporter/ Manipulator System (ATMS). The configuration of the computer hardware is illustrated below.

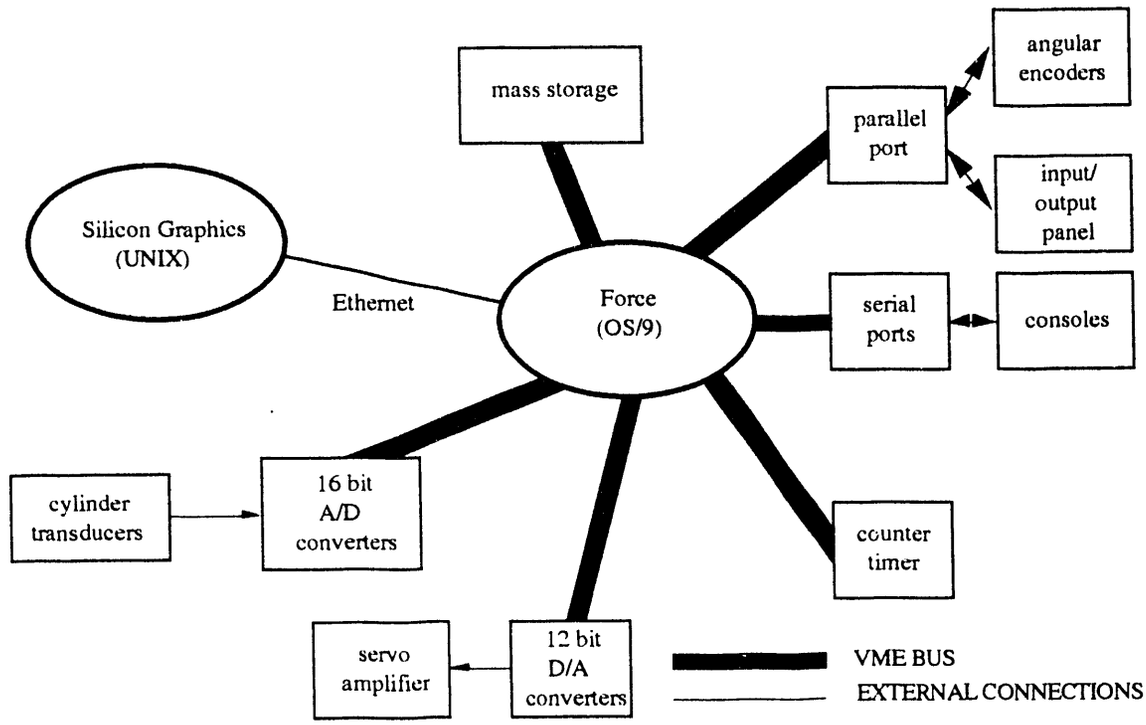

The control system hardware consisted of a Force computer running the OS/9 real-time operating system and a Silicon Graphics computer running Unix. The Force computer consisted of a central processing unit and several input and output boards utilized for transmitting and receiving information to and from the environment. Analog to digital converters quantified linear position of the hydraulic cylinders. The voltage signals from transducers mounted inside the hydraulic cylinders were converted to cylinder lengths. Servo-amplifiers were utilized to convert a voltage signal from digital to analog channels to a current signal for the servo-valves. The servo-valve spool moved in response to the current; effecting motion by supplying hydraulic pressure to

the hydraulic cylinders. Serial ports were utilized for communications between the central processing unit and the operator. A parallel port was utilized to interface angular encoders, control power to devices, and sense the power status of devices for safety purposes. An input/output panel optically coupled two 8 bit ports of the parallel board. Solid state relays were used to sense and control the power status to several devices. Four solid state relays provided 120 VAC power to ± 15 and ± 5 VDC power supplies, the servo-amplifier, and the hydraulic dump valve. Status of 120 VAC power to several devices were detected using AC sense modules for safety reasons. Helix software utilized the Ethernet line between the Silicon Graphics and the Force to communicate information between the two systems. At present, a graphic program developed on the Silicon Graphics computer allowed the user to alter the desired linear length and rotational angle of the ATMS test bed. Development of path planning software is not covered in this section of this report.

The operating environment is shown graphically in the following figure. The operating environment was divided into the work environment, an operating system, an operating language, debugging facilities, and path planning. The operating system included a scheduler and the input and output software and hardware. Input and output modules were used to interface the computer system to the work environment. The operating language was used to indicate modes of operation. During development, it was required to operate the ATMS test bed in many different operational modes. Examples of different modes were open-loop control, closed-loop control, and Silicon Graphics control of body length and angle. The operating language provided the flexibility to alter the operational mode without recompiling software code. The language consisted of models and a state network. Models characterized events occurring in the environment by mapping sensor data to binary results. While input drivers mapped infinitely variable environmental quantities to finite numerical results, the data sets were too large to be handled efficiently. The state network consisted of a linked list of the desired operational modes for the ATMS. Path planning software on the Silicon Graphics would generate commands for the ATMS to obey.

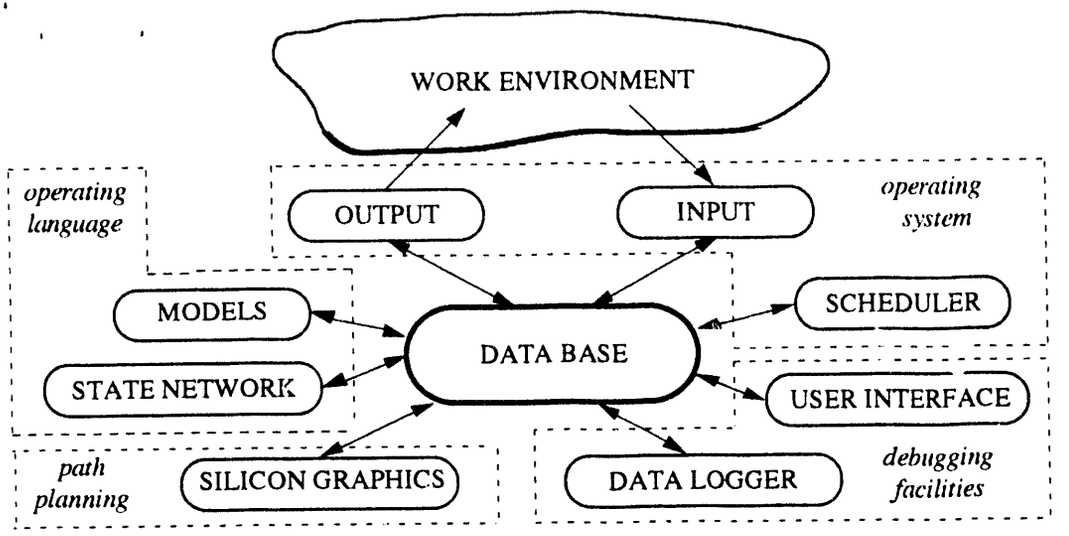

Input and output software drivers were developed to quantify the environment. A diagram of a typical input driver is shown below. In this example, a linear transducer in a hydraulic cylinder was used to sense the stroke of the cylinder. The joint position input driver used an analog to digital converter to map the transducer voltage into a cylinder position and stored the result in the data base.

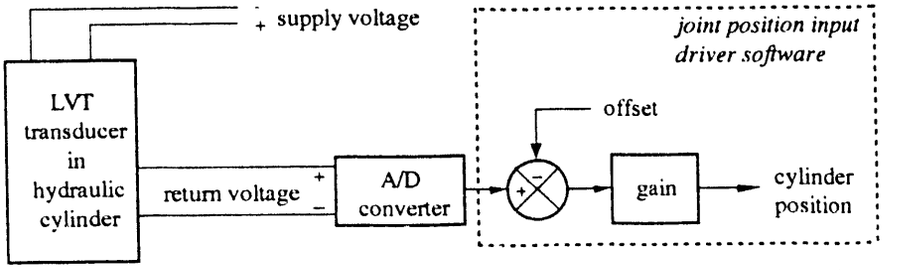

An example of an output software driver is shown below. In this example, a desired position set point is used with the actual position of the cylinder to generate an error signal. The error signal was converted by a digital to analog converter channel to an analog voltage. The servo-amplifier converted this voltage to a current signal proportional to the voltage and delivered the signal to the servo-valve. Changes to the servo-valve spool position results in movement of a hydraulic cylinder.

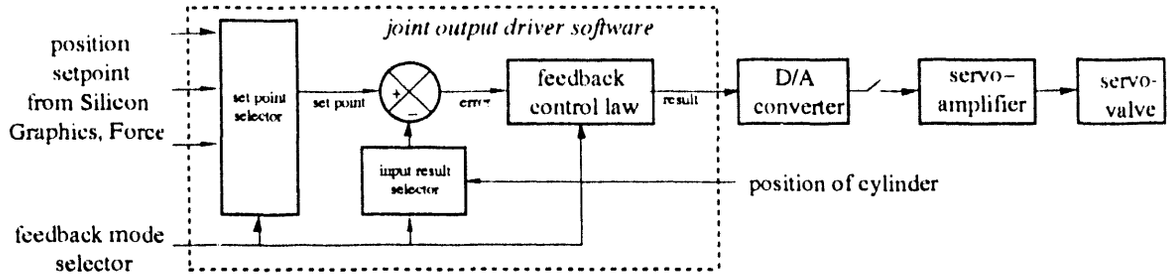

Hydraulic power is delivered to the ATMS test stand by a hydraulic power unit (HPU). A schematic of the HPU is shown below. A hydraulic schematic for a hydraulic cylinder follows.

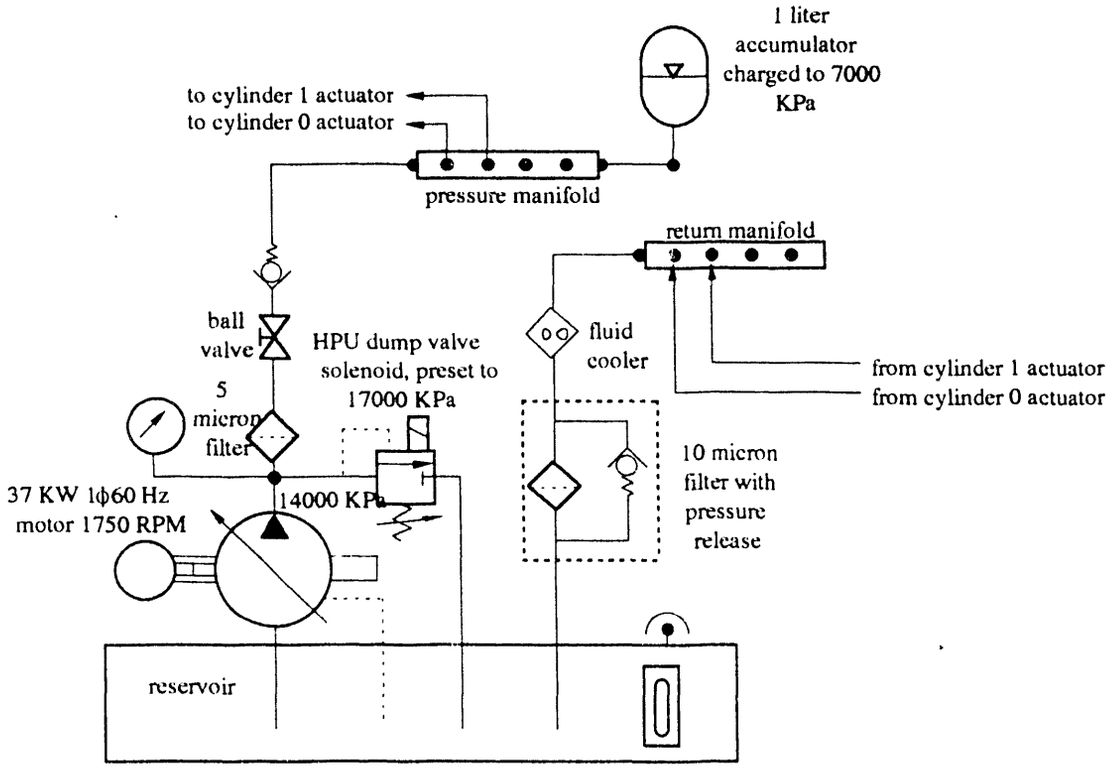

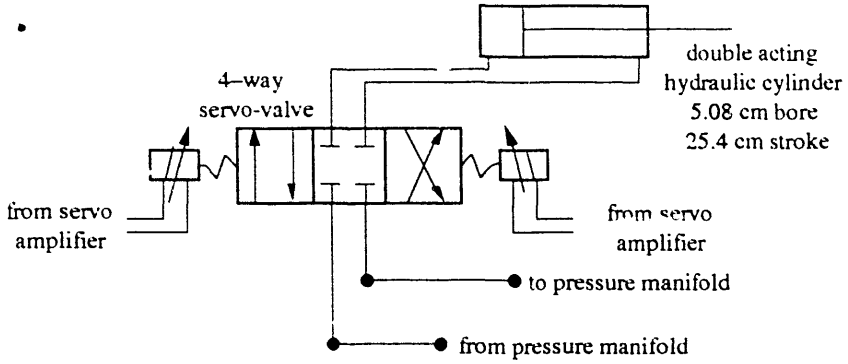

Sensing power to devices was the responsibility of a power input driver. For example, computer and user control of a dump valve in the hydraulic power unit circuit provided an element of safety. A schematic of the dump valve electrical circuit is shown below. The parallel port connected to an input/output board provided the ability to switch 120 VAC power to the dump valve and detect 120 VAC power at the dump valve. If the external push button is open, power is lost at the dump valve. The computer sensed the loss of power and took proper action to bring the ATMS to a home configuration.

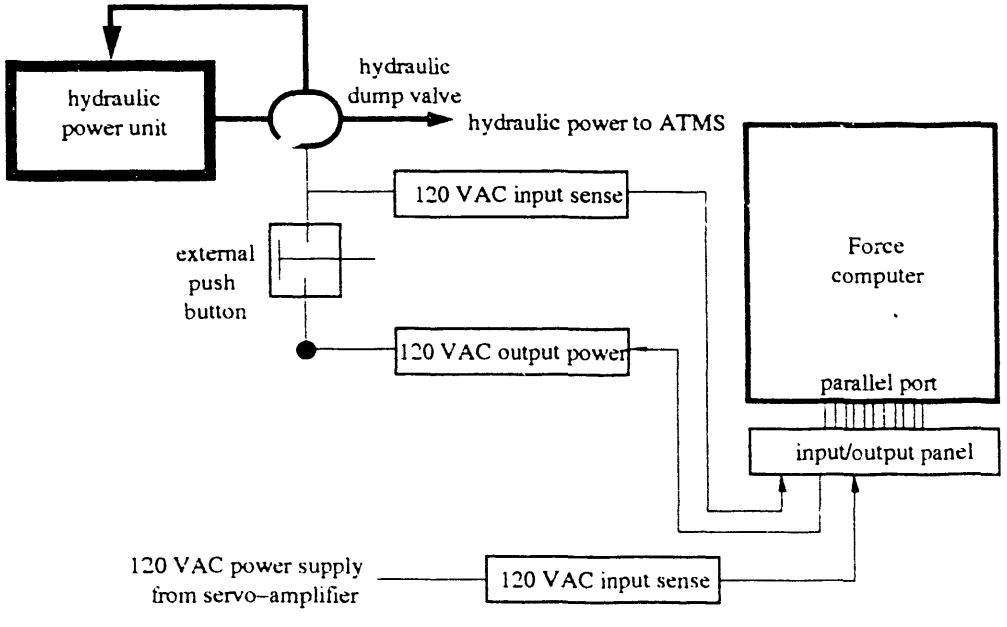

Intelligent operation of the ATMS required the ability to sense the environment, make intelligent decisions, and output information to actuation devices. The data base represented a structure which provided asynchronous data exchange among different software components. This provided a method of data exchange between I/O driver software and the operating language. This was accomplished by reserving a section of computer memory for global information storage. Input hardware and driver software were programmed to acquire sensor information from the environment. Output hardware and driver software calculated and sent information to actuation devices. Both input and output driver software utilized sections of the data base memory to store information.

A scheduler was developed to activate input and output drivers, models, the state network and the data logger. The scheduler was executed at a real-time rate of 100 Hz. After input drivers acquired sensor information, models were activated to quantify the sensor data. The state network was examined to determine if a mode change was indicated. After these components had completed execution, the output drivers were activated to transfer information to actuation devices.

The user interface provided a window into the system. The user interface was a command driven program that allowed the user to type commands to alter or examine parameters in the data base. A data logger program could be activated to record 30 seconds of real-time data in a circular que. The data could be down loaded to a graphical plotting routine on a Macintosh computer that served as a console. In this manner, tests on the ATMS test bed could be performed and analyzed.

Open-loop and closed-loop testing on the ATMS test stand are now commencing. Open-loop natural frequencies of approximately 6-8 Hz. are common with damping ratios ranging from 0.1 to 0.5. A plot of an open-loop test of cylinder 0 is shown on the next page. A variety of closed-loop feedback control laws are being examined to determine which are suitable for given positional accuracies. A plot of a closed-loop test of cylinder 1 is also shown. Two general schemes of controlling the hydraulic cylinders will be examined. These deal with the location of sensor feedback from the ATMS segment. If the length of each cylinder is known (position sensor on or in hydraulic cylinder), a desired position set point for each cylinder can be calculated from

the desired body length and angle. Position control of the hydraulic cylinders would be straight forward with this configuration. The other scheme is to directly feedback the body length and angle of an ATMS segment. With this scheme, the lengths of each hydraulic cylinder would not be known explicitly. This control strategy being investigated is shown in the figure following the open and closed-loop test plots. Advantages of controlling the body length and angle rather than controlling the length of each hydraulic cylinder include cost savings and ease of sensor replacement and maintenance.

Open loop test of cylinder 0

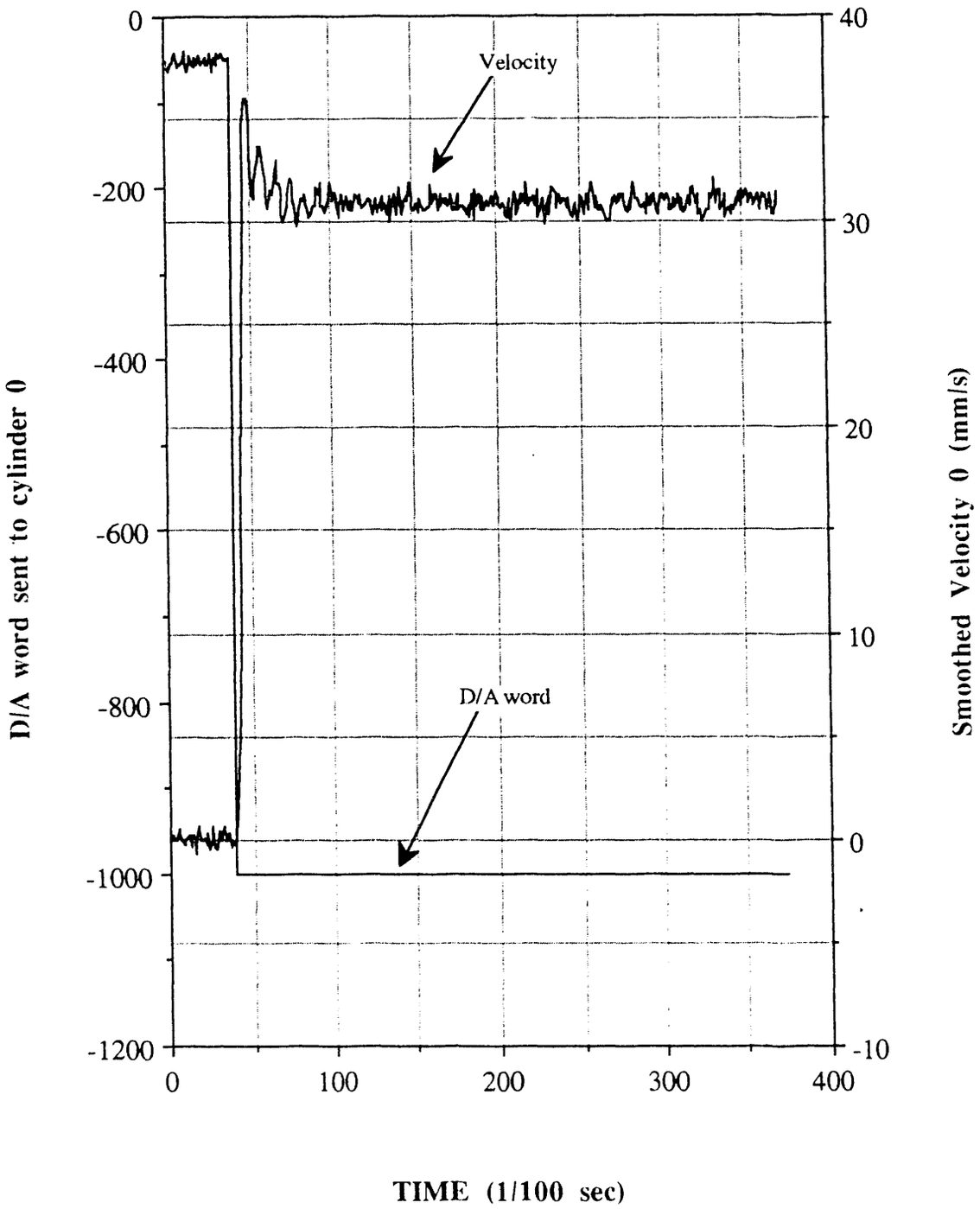

Closed loop step test of cylinder 1

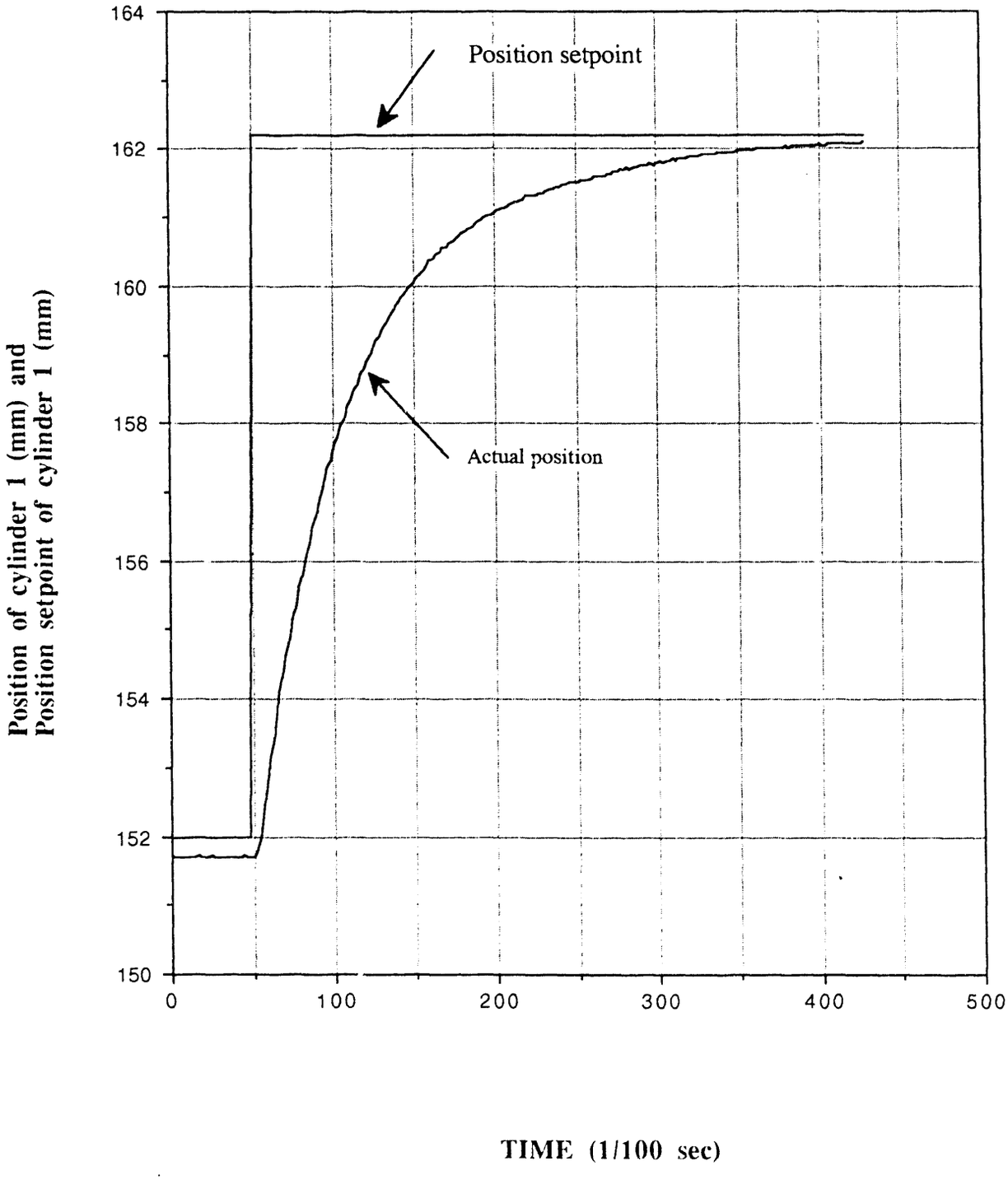

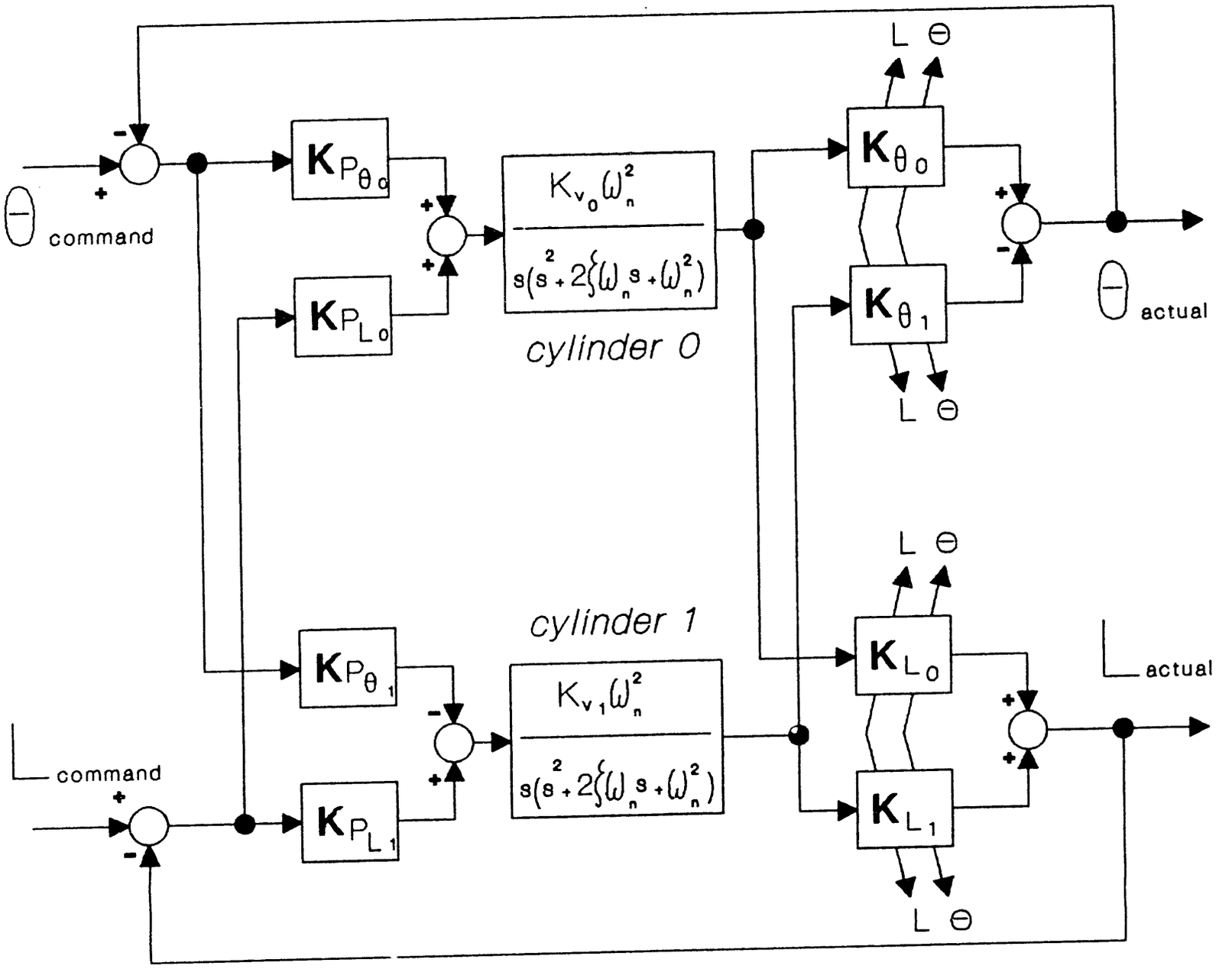
command
$K_{P\theta_0}$
K_{PL_0}
$\frac{K_{v_0}\omega_n^2}{s(s^2+2\zeta\omega_n s+\omega_n^2)}$
cylinder 0
K_{θ_0}
K_{θ_1}
L Θ
L Θ
actual
cylinder 1
$K_{P\theta_1}$
K_{PL_1}
$\frac{K_{v_1}\omega_n^2}{s(s^2+2\zeta\omega_n s+\omega_n^2)}$
K_{L_0}
K_{L_1}
L Θ
L Θ
command
actual

1.0 ENVIRONMENTAL HARDENING:

During the reporting period of 1991, the research on environmental hardening of electronic components was concentrated on two subtasks. First, the test facility was to be upgraded to an On-line Testing and Feedback Radiation Facility. Secondly, the chip for computer control of the Cybermotion Robot Sensing System was to be radiation hardened allowing it to survive longer in a radiation field.

1.1 ON-LINE TESTING AND FEEDBACK RADIATION FACILITY:

The tests are carried out in a Cobalt 60 irradiator, shown in Figure 1.1.1, which has a current source strength of 400 curies, a working volume 33.5 cm high x 38.7 cm wide x 44.4 cm deep and a dose rate to our specimens of about 1/2 Krad/min.

The on-line monitoring system has been made operational in the testing facility. The idea behind the on-line system is to operate the MC68008 in a mode that does not execute any code with all address lines floating. The net result is that address line (AO) toggles from a low to high state each time the program counter is incremented by one. Thus a constant frequency square wave is seen at AO. Any deviation above the tolerance limit indicates failure.

Since the irradiation usually extends over long periods of time, it is not possible to manually keep track of frequency changes. A complete on-line monitoring system has thus been developed and makes use of an acquisition card and a personal computer. The acquisition card has been set in the frequency measuring mode and the computer's software detects any deviations in the frequency above the predetermined limits.

The first part of the experiment involves the calibration of the chip when a statistical file is generated regarding the particular chip. The procedure takes around 45 minutes and can be done any time before the irradiation experiment. When the experiment begins, the software reads

END

DATE
FILMED
2/03/92